Organoaluminium complexes derived from Anilines or Schiff bases for ring opening polymerization of ε-caprolactone, δ-valerolactone and *rac*-lactide

Xue Wang,[a] Ke-Qing Zhao,[a] Yahya Al-Khafaji,[b] Shangyan Mo,[b] Timothy J. Prior,[b] Mark R. J. Elsegood[c] and Carl Redshaw[a,b*]

[a] College of Chemistry and Materials Science, Sichuan Normal University, Chengdu, 610066, China.

[b] Department of Chemistry, University of Hull, Hull, HU6 7RX, U.K.

[c] Chemistry Department, Loughborough University, Loughborough, Leicestershire, LE11 3TU, U.K.

Abstract: Reaction of $R^1R^2CHN=CH(3,5-tBu_2C_6H_2-OH-2)$ ($R^1 = R^2 = Me$ **L¹H**; $R^1 = Me$, $R^2 = Ph$ **L²H**; $R^1 = R^2 = Ph$ **L³H**) with slightly greater than one equivalent of R^3_3Al ($R^3 = Me$, Et) afforded the complexes $[(L^{1-3})AlR^3_2]$ (L^1, $R^3 = Me$ **1**, $R^3 = Et$ **2**; L^2, $R^3 = Me$ **3**, $R^3 = Et$ **4**; L^3 $R^3 = Me$ **5**, $R^3 = Et$ **6**); complex **1** has been previously reported. Use of the *N,O*-ligand derived from 2,2′-diphenylglycine afforded either **5** or an amine by-product $[Ph_2NCH_2(3,5-tBu_2C_6H_2-O-2)AlMe_2]$ (**7**). The known Schiff base complex $[2-Ph_2PC_6H_4CH_2(3,5-tBu_2C_6H_2-O-2)AlMe_2]$ (**8**) and the product of the reaction of 2-diphenylphosphinoaniline $1-NH_2,2-PPh_2C_6H_4$ with Me_3Al, namely $\{Ph_2PC_6H_4N[(Me_2Al)_2\mu-Me](\mu-Me_2Al)\}$ (**9**) were also isolated. For structural and catalytic comparisons, complexes resulting from interaction of Me_3Al with diphenylamine or benzhydrylamine, namely $\{Ph_2N[(Me_2Al)_2\mu-Me]\}$ (**10**) and $[Ph_2CHNH(\mu-Me_2Al)]_2\cdot MeCN$ (**11**), were prepared. The molecular structures of the Schiff pro-ligands derived from Ph_2CHNH_2 and $2,2′-Ph_2C(CO_2H)(NH_2)$, together with complexes **5**, **7** and **9** - **11·MeCN** were determined; **5** contains a chelating imino/phenoxide ligand, whereas **7** contains an amine/phenoxide ligand. Complex **9** contains three nitrogen-bound Al centres, two of which are linked via a methyl bridge, whilst the third bridges the N and P centres. In **10**, the structure resembles **9** with a bridging methyl group, whereas the introduction of the extra carbon in **11** results in the formation of a dimer. All complexes have been screened for their ability to ring opening polymerization (ROP) ε-caprolactone, δ-valerolactone or *rac*-lactide, in the presence of benzyl alcohol, with or without solvent present. Reasonable conversions were achievable at room temperature for ε-caprolactone using complexes **7**, **9** and **12**, whilst at higher temperatures (80 – 110 °C), all complexes produced good (> 65%) to quantitative conversions over periods as short as 3 min. albeit with poor control. In the absence of solvent, conversions were near quantitative at 80 °C over 5 min. with better agreement between observed and calculated molecular weight (M_n). For *rac*-lactide, conversions were typically in the range 71 – 86% at 110 °C over 12 h, with poor control affording atactic polylactide (PLA), whilst for δ-valerolactone more forcing conditions (12 - 24 h at 110 °C) were required for high conversion. Co-polymerization of ε-caprolactone with *rac*-lactide afforded co-polymers with appreciable lactide content (35 – 62.5%); the

reverse addition was ineffective affording only (polycaprolactone) PCL.
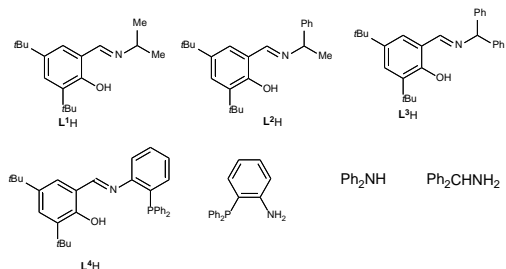
Introduction

The use of ring opening polymerization (ROP) of cyclic esters remains a topical area given the ease of access to a range of biodegradable polymers.[1] The polymer products have wide potential, finding use in, for example, the packaging industry as well in the biomedical field (e.g. as implants).[2] Of the complexes employed as catalysts in such ROP reactions, aluminium species, given both their low toxicity and high Lewis acidity, continue to attract the interest of a number of research groups.[3] For alkylaluminium complexes, the addition of an alcohol, typically benzyl alcohol or isopropanol, generates the required catalytic alkoxide species. Easily prepared pro-ligands are also a prerequisite if such systems are to be employed on a bulk scale. With this in mind, the use of phenoxyimine type ligation has attracted interest, and a number of structure/activity relationships have been identified.[4] Indeed, a search of the CSD revealed 343 hits for dialkylaluminium where N and O complete the coordination environment, and of these hits, 76 contained chelating phenoxyimine ligand sets.[5] For an overview of the phenoxyimine aluminium systems that have previously been employed in the ROP of cyclic esters, see Table S1 (SI).[6, 7] Having employed this type of ligand set recently in vanadium-based α-olefin polymerization,[8] we now, as part of our continued interest in designing new aluminium-based initiators/catalysts for the ROP of cyclic esters,[6t] report our results on the series of complexes $[R^1R^2CHN=CH(3,5-tBu_2C_6H_2-O-2)AlMe_2]$ ($R^1 = R^2 = R^3 = Me$ **1**; $R^1 = R^2 = R^3 = Et$ **2**; $R^1 = R^3 = Me$, $R^2 = Ph$ **3**; $R^1 = Me$, $R^2 = Ph$, $R^3 = Et$ **4**; $R^1 = R^2 = Ph$, $R^3 = Me$ **5**; $R^1 = R^2 = Ph$, $R^3 = Et$ **6**) and compare their behaviour against organoaluminium complexes derived from the amine component only (*i.e.* minus the phenoxy-containing 3,5-di-*tert*-butylsalicyl motif, see Schemes 1 and 2). We note that Nomura has previously investigated the effect of the imino substituent on the ROP of ε-CL, and observed greatly enhanced activity for aryl substituents (C_6F_5, 2,6-iPr$_2$C$_6$H$_3$) *versus* aliphatic substituents (adamantyl, *tert*-butyl).[7] Herein, we initially targeted diphenylglycine and derivatives thereof given the tendency of related motifs to form highly crystalline products.[9] However, the loss of CO_2 during the formation **L³**H (dpg), see discussion below, led us to explore the family of pro-ligands with both aliphatic and aromatic substituents bound to the N-bound CH group.
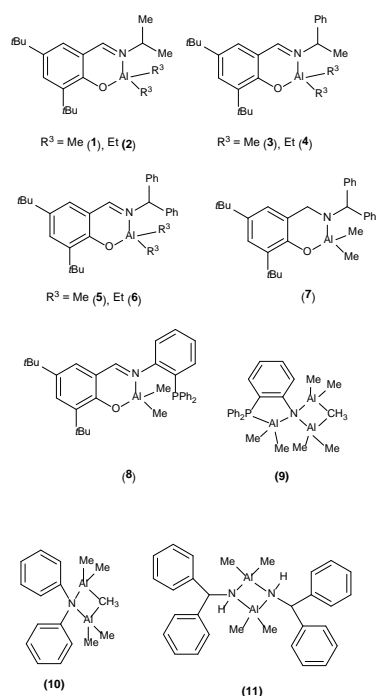
Results and Discussion

Pro-ligands $L^{1-5}H$

The Schiff-base pro-ligands used herein were prepared by standard condensation procedures in good yields > 90% except in the case of **L³**dpg (63%).[10]

Scheme 1. Compounds (pro-ligands) employed herein.

R³ = Me (**1**), Et (**2**)   R³ = Me (**3**), Et (**4**)

R³ = Me (**5**), Et (**6**)   (**7**)

(**8**)   (**9**)

(**10**)   (**11**)

Scheme 2. Complexes studied herein

The IR spectra contained a relatively strong ν(C=N) band at *ca.* 1628 cm^{-1}, whilst in the ^{1}H NMR spectrum, δ OH typically appeared at 13.68 ppm. The pro-ligands $\mathbf{L^1}$H and $\mathbf{L^4}$H have been previously reported.[10,11] Crystals suitable for single crystal X-ray diffraction of $\mathbf{L^3}$H (dpa), obtained via the use of benzhydrylamine (dpa) were grown from a saturated acetonitrile solution at ambient temperature. The molecular structure is shown in Figure 1, with selected bond lengths and angles given in the caption. There are two unique molecules in the asymmetric unit with

slightly different arrangement of the phenyl groups and methyl groups. In each of the two molecules the core is essentially planar; there is an intramolecular hydrogen bond between the phenol and the imine groups.
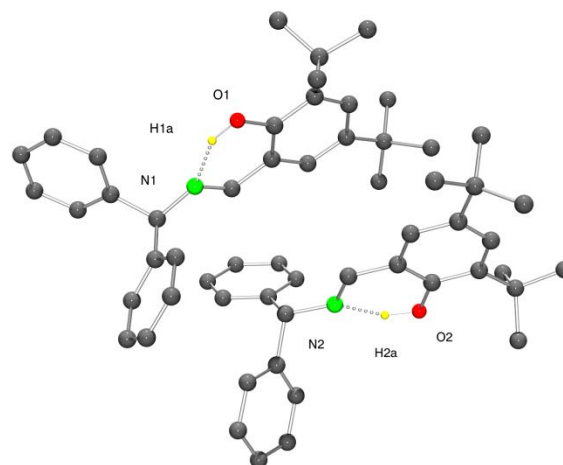

Figure 1. Representation of the asymmetric unit of $\mathbf{L^3}$H (dpa). Hydrogen atoms attached to carbon have been omitted for clarity. Dashed lines indicate intramolecular hydrogen bonds. Selected bond lengths (Å) and angles (°): O1–H1A 0.96(4), O1···N1 2.602(3), O2–H2A 1.02(4), O2···N2 2.597(3) Å; O1–H1A···N1 149(4), O2–H2A···N2 154(3).

The packing of the molecules is largely unremarkable. There is some evidence of short C–H···π distances (e.g. H15 lies approximately 2.80 Å above the plane of ring C31–C36; H35 lies approximately 2.95 Å from the plane of ring C3^i–C8^I [i = 1=x, y, z]).

Similar use of diphenylglycine (dpg), 2,2′-Ph₂C(CO₂H)(NH₂), resulted in loss of CO₂ during the conditions employed herein and formation of a pale yellow product. A crystal structure determination revealed that the structure of $\mathbf{L^3}$H (dpg) was identical to that obtained using dpa (see Fig. S1 in the SI for overlap of the

structures and Fig. S2 for the molecular structure and bond lengths and angles for **L³H** (dpg)). A phase change accounts for the differing unit cells in Table 7 which were collected at 150 and 293 K.

Organoaluminium complexes


Scheme 3. Synthesis of complexes **1 - 6**
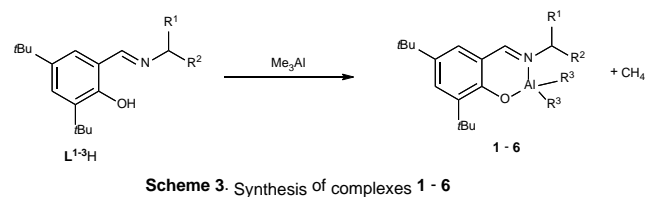
Reaction with 1.1 equivalents of Me₃Al with the parent Schiff bases in refluxing toluene afforded, after work-up, moderate to good yields (55 – 97%) of the complexes [$R^1R^2CHN=CH(3,5-tBu_2C_6H_2$-O-2)$AlMe_2$] ($R^1 = R^2 = R^3 =$ Me **1**; $R^1 = R^2 = R^3 =$ Et **2**; $R^1 = R^3 =$ Me, $R^2 =$ Ph **3**; $R^1 =$ Me, $R^2 =$ Ph, $R^3 =$ Et **4**; $R^1 = R^2 =$ Ph, $R^3 =$ Me **5**; $R^1 = R^2 =$ Ph, $R^3 =$ Et **6**), see scheme 3. Complex **1** was previously reported by Milione *et al*, and used for halide anion binding via H-bonding,[11] whilst the debutylated version of complex **5** has recently been employed by Chiang, Chen and Chen and coworkers for the ROP of ε-caprolactone and *L*-lactide; the structure of debutylated **5** was not reported.[6z] Herein, crystals of **5** suitable for an X-ray diffraction study were grown from acetonitrile on prolonged standing at ambient temperature. The molecular structure is shown in Figure 2 with selected bond lengths and angles given in the caption; crystallographic data are presented in Table 2.

The asymmetric unit of **5** contains one molecule of the complex; there is no solvent of crystallization. The C–N bond at 1.32(3) Å is consistent with an imine linkage, whilst the Al–N bond length (1.98(2) Å) is typical of reported Al–N imine bonds.[12] In the packing of the complex, the structure adopted is layered, with C–H···π interactions between layers.
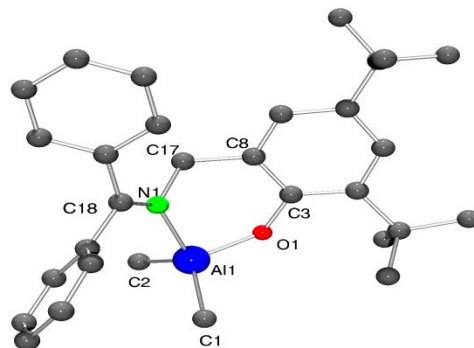
Figure 2. Molecular structure of [$Ph_2CHN=CH(3,5-tBu_2C_6H_2$-O-2)$AlMe_2$] (**5**), showing the atom numbering scheme. Hydrogen atoms have been omitted for clarity. Selected bond lengths (Å) and angles (°): Al(1)–O(1) 1.769(11), Al(1)–N(1) 1.991(14), Al(1)–C(1) 1.965(16), Al(1)–C(2) 2.04(2), N(1)–C(17) 1.317(19), N(1)–C(18) 1.522(19), C(8)–C(17) 1.50(2); O(1)–Al(1)–N(1) 92.5(6), C(1)–Al(1)–C(2) 118.0(10), Al(1)–O(1)–C(3) 125.7(11), Al(1)–N(1)–C(18) 126.0(9).
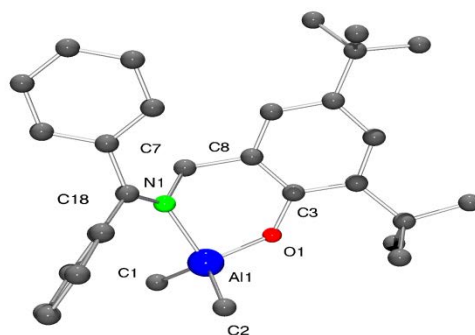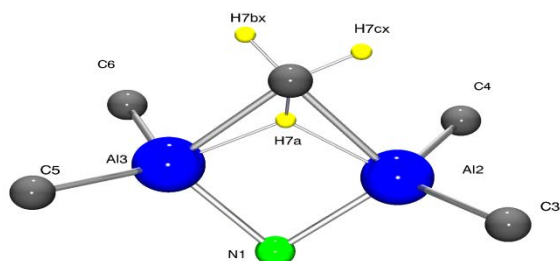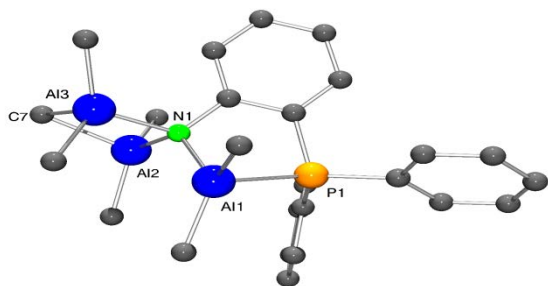

Figure 3. Molecular structure of [$Ph_2CHNCH_2(3,5-tBu_2C_6H_2$-O-2)$AlMe_2$] (**7**), showing the atom numbering scheme. Hydrogen atoms and non-coordinated solvent molecules have been omitted for clarity. Selected bond lengths (Å) and angles (°): Al(1)–O(1) 1.7675(11), Al(1)–N(1) 2.0088(13), Al(1)–C(1) 1.9636(17), Al(1)–C(2) 1.9537(16), N(1)–

C(17) 1.4900(17), N(1)–C(18) 1.2894(19), C(8)–C(17) 1.512(2); O(1)–Al(1)–N(1) 94.06(5), C(1)–Al(1)–C(2) 119.65(8), Al(1)–O(1)–C(3) 129.65(9), Al(1)–N(1)–C(18) 129.57(10).

On one occasion, we also isolated the amine complex [Ph$_2$NCH$_2$(3,5-tBu$_2$C$_6$H$_2$-O-2)AlMe$_2$] (**7**), the molecular structure of which is shown in Figure 3. The longer Al–N and N–C bond lengths are consistent with an amine linkage.[13] The nitrogen N(1) is not protonated here as the sum of the angles is 360° and planar (i.e. not pyramidal), whilst N(1) – C(18) is 1.29 Å (double bond) and N(1) – C(17) is 1.49 Å (single bond). The situation is reminiscent of that reported for the amine nitrogen in the complex {MoCl(NtBu)[1-μ(N),2-(Ph$_2$P)C$_6$H$_4$]}$_2$.[13a] The formation of **7** is thought to be due to the presence of excess Me$_3$Al acting as a reducing agent. Interestingly, Stephan *et al* have recently reported imine hydrogenation by alkylaluminium catalysts (eg iBu$_3$Al) albeit under more forcing conditions; a hydroalumination/hydrogenolysis mechanism was invoked.[14]

For comparative ROP studies (see later), we also prepared the known Schiff base complex [2-Ph$_2$PC$_6$H$_4$CH$_2$(3,5-tBu$_2$C$_6$H$_2$-O-2)AlMe$_2$] (**8**),[10] and studied the interaction of 2-diphenylphosphinoaniline, 1-NH$_2$,2-PPh$_2$C$_6$H$_4$, with an excess of Me$_3$Al. In the case of diphenylphosphinoaniline, following work-up, small colourless crystals suitable for X-ray diffraction using synchrotron radiation were isolated in 56% yield.[15] As shown in Figure 4, the complex (**9**) contains three tetrahedral dimethylaluminium centres, two of which are bound to what was the amino nitrogen N(1), and also to each other via a methyl bridge. A search of the CSD revealed 30 hits for methyl bridging of aluminium centres (see Chart S1, SI).[16, 17] In **9**, two out of three H atoms on the CH$_3$ group at C(7) are disordered. In the difference electron density map, one clear peak is seen with a peak height of *ca*. 0.9 eÅ^{-3} which is refined fully occupied as H(7A). There are also *ca*. four smaller peaks of between 0.4-0.5 eÅ^{-3} which are refined in pairs as the other bridging methyl H atoms. The third aluminium centre Al(1) bridges N(1) and P(1). The structure is reminiscent of [(Me$_2$Al)$_2$(μ-Me)(μ-NPh$_2$)] (**I**, see top chart S1, SI), obtained via the reaction between diphenylamine and Me$_3$Al.[16b] In **I**, the three H atoms were modelled as all pointing away from the Al–C bonds, i.e. no equivalent of the H(7A) atom in **9**. The Al–C bond lengths {2.145(5) and 2.139(5) in **I** and 2.176(3) and 2.146(3) Å in **9**} and Al–C–Al angle {78.92(17) in **I** and 77.40(11) ° in **9**} are, however, remarkably similar. Mild geometrical restraints were applied to make all the C(7)–H distances similar, and also to keep the H···H distances similar for the pairs of disordered H atoms. While a model could be refined with restraints for all three H atoms pointing away, there remained the large peak nearer the Al atoms, and the *R* factor was worse. The two approximately trigonal planar disorder components are approximately 90° apart, with the minor disorder {48(4)% occupancy) component being less planar than the major. There is no solvent of crystallization in **9**.

Figure 4. Top: Molecular structure of {Ph$_2$PC$_6$H$_4$N[(Me$_2$Al)$_2$μ-CH$_3$](μ-Me$_2$Al)} (**9**), showing the atom numbering scheme. Bottom: Structure around Al(2) and Al(3) core. Selected bond lengths (Å) and angles (°): Al(1)–N(1) 1.9432(19), Al(1)–P(1) 2.4481(9), Al(2)–N(1) 1.9465(18), Al(2)–C(7) 2.176(3), Al(3)–N(1) 1.9551(18), Al(3)–C(7) 2.146(3), Al(1)–Al(2) 3.4374(10), Al(2)–Al(3) 2.7022(10); N(1)–Al(1)–P(1) 83.76(6), Al(2)–C(7)–Al(3) 77.40(11), Al(2)–N(1)–Al(3) 87.67(7).

Given the nature of the bridging methyl group in **9** *versus* that reported for **I**,[16b] we decided to re-examine the structure of the diphenylamine derived aluminium structure. Single crystals of **10** suitable for X-ray diffraction were grown from hexane in *ca* 63% yield, which proved to be a two component twin with domains related by a 180 ° rotation about real and reciprocal axes 010. There is one molecule of **10** in the asymmetric unit (no solvent of crystallization), which is shown in Figure 5 with selected bond lengths and angles given in the caption.
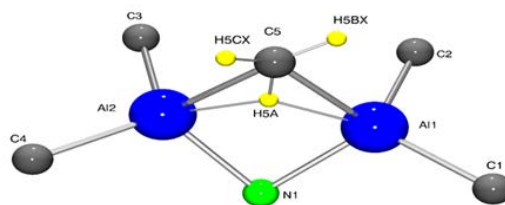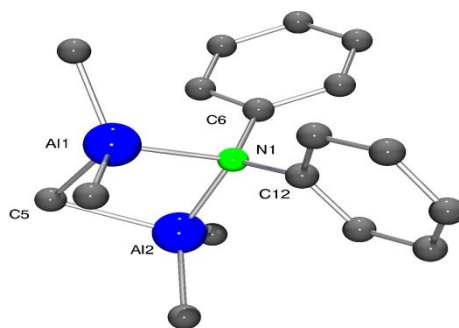
Figure 5. Top: Molecular structure of {Ph$_2$N[(Me$_2$Al)$_2$μ-Me]} (**10**), showing the atom numbering scheme. Bottom: Structure around Al(1) and Al(2) core. Selected bond lengths (Å) and angles (°): Al(1)–N(1) 2.0014(18), Al(2)–N(1) 1.9944(18), Al(1)–C(5) 1.957(2), Al(2)–C(5) 2.145(2); Al(1)–N(1)–Al(2) 85.90(7), Al(1)–C(5)–Al(2) 78.77(8), C(6)–N(1)–C(12) 113.15(15).

The group at C(5) tallies with the conclusion for **I**. The Al$_2$NC butterfly in **10** has a shallow hinge angle of 28.24(10)°, which is somewhat shallower than that observed in **9** at 15.19(18)°. Again, VSEPR theory suggests this centre should be trigonal planar. We note that in **I**, the three H atoms are modelled as all pointing away from the Al–C bonds, i.e. no equivalent of the H(7A) atom in **9** or the H(5A) atom in **10**. The Al–C bond lengths {2.145(5) and 2.139(5) in **I**, 2.176(3) and 2.146(3) in **9**, and 2.145(2) and 2.146(2) Å in **10**} and Al–C–Al angle {78.92(17) in **I**, 77.40(11) in **9**, and 78.77(8)° in **10**} are, however, remarkably

similar. Mild geometrical restraints were applied to make all the C(5)–H distances similar, and also to keep the H···H distances similar for the pairs of disordered H atoms. While a model could be refined with restraints for all three H atoms pointing away, there remained the large peak nearer the Al atoms, and again the R factor was worse. The two approximately trigonal planar disorder components are approximately 90° apart, with the minor disorder {47(4)% occupancy) component being less planar than the major. One electron density peak remained approximately 180° away from H(5A).

Introduction of an extra carbon in the form of benzhydrylamine and subsequent treatment with two equivalents of Me_3Al led to the formation of $[Ph_2CHNH(\mu-Me_2Al)]_2 \cdot MeCN$ (**11·MeCN**) in moderate yield (47%). Single crystals were grown from a saturated acetonitrile solution on prolonged standing (12 h) at 0 °C. The molecular structure is shown in Figure 6; selected bond lengths and angles given in the caption. One Al dimer and one MeCN of crystallization comprise the asymmetric unit. The Al_2N_2 core adopts a shallow butterfly shape with a dihedral angle of 9.66(6)°. Interestingly, the geometrical parameters associated with the Al_2N_2 square are somewhat of a hybrid of those observed for the anisidine derived complexes {[1,2-(OMe),N-$C_6H_4(\mu-Me_2Al)](\mu-Me_2Al)}_2$, [1,3-(Me_3AlOMe),NH-C_6H_4(\mu-Me_2Al)]_2$ and [1,4-(Me_3AlOMe),NH-C_6H_4(\mu-Me_2Al)]_2$ and the pyrrolyl-methylamide complexes {[C_4H_3N(2-CH_2HtBu)]AlH}_2$ and {[C_6H_3N(2-CH_2HtBu)]Al(OCHMe_2)}_2$ in that the Al–N bond lengths are *ca*. 1.96 Å (found in the 1,4-anisidine

derived complex and the pyrrolyl-methylamide), whilst the angles are *ca*. 88 ° (found in the1,2/1,3-anisidine derived complexes).[18] In **11·MeCN**, both N–H groups point 'up', and there is one, well-behaved MeCN solvent molecule of crystallization which is H-bonded to one of the two N–H moieties; the dimensions associated with the H-bonding are given in the SI (Table S2).
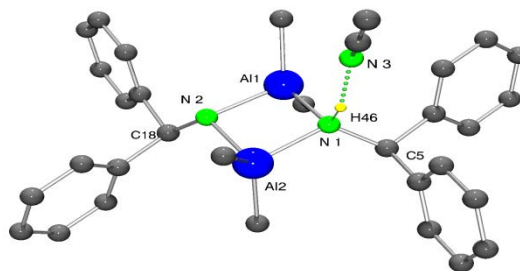

Figure 6. Molecular structure of [Ph_2CHNH(μ-Me_2Al)]_2·MeCN (**11·MeCN**), showing the atom numbering scheme. Most hydrogen atoms have been omitted for clarity. Selected bond lengths (Å) and angles (°): Al(1)–N(1) 1.9597(10), Al(1)–N(2) 1.9484(10), Al(2)–N(1) 1.9620(10), Al(2)–N(2) 1.9528(10), N(1)–C(5) 1.4771(14), N(2)–C(18) 1.4836(13); Al(1)–N(1)–Al(2) 91.72(4); Al(1)–N(2)–Al(2) 92.35(4), N(1)–Al(1)–N(2) 86.67(4), N(1)–Al(2)–N(2) 87.48(4).

Ring Opening Polymerization (ROP) of ε-Caprolactone (ε-CL)
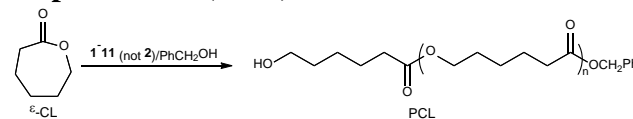
Scheme 4. ROP of ε-CL

Given that aluminium compounds are known to be efficient catalysts for ring opening polymerization (ROP) of cyclic esters,[3] the catalytic behavior of **1 - 11** was explored toward the ROP of ε-CL in the presence of benzyl alcohol (BnOH), scheme 4. One equivalent (per aluminium) of BnOH were employed in the runs

herein. Despite the apparent mismatch of stoichiometry, the use of one equivalent of BnOH (per aluminium) for R_2Al containing pre-catalysts is well established; the use of two equivalents (per aluminium) has been found to afford inferior results.[6a,c,e] In our systems, extending the reaction time (see Table S3) or varying the amount of BnOH was not found to be beneficial. Pre-catalyst **2** was employed to ascertain the optimum conditions (see Table S4), and was found to be effective for the ROP of ε-CL at temperatures of 80 to 110 $^{\circ}$C affording conversions > 67%. According to the entries (1-5), there is an exponential relationship between monomer conversions and M_n values, possibly due to severe catalyst decomposition, with molecular weight distributions [1.08 – 2.14] that suggest there is some degree of control. A linear relationship between [CL]/[Al] ratio and average molecular weight (M_n), suggests the systems still retain the classical features of a living polymerization process (Figs. S3 and S4, SI). Elevation of the temperature generally resulted in higher molecular weight polymer and high conversion (Fig. S5, SI) with an increase in the monomer/Al ratio from 62.5:1 to 1000:1 at 110 $^{\circ}$C, the molecular weight increased from 3.1×10^3 to 38.5×10^3, with little change of PDI (1.23 - 2.08), but producing polymers with lower molecular weight than the calculated M_n values. Prolonging the reaction time to 12 h (runs 8 and 9) led to decreased conversions rates, presumably due to catalyst decomposition; at 110 $^{\circ}$C in toluene$_8$ in a sealed NMR tube, the spectrum reveals distinct changes even after 1 h.

In addition, we investigated the behaviour of the other complexes herein towards the ROP of ε-CL, using the ratio 250:1:1 (see Table 1). Generally, these aluminium complexes displayed good catalytic conversions, particularly at temperatures of 80 $^{\circ}$C or higher (> 92%). Catalytic systems employing complexes **7**, **9**, **10** and **11** outperformed the others at 110 $^{\circ}$C, affording quantitative conversions over 13 mins or less. For complexes **1** - **6**, the trend is for the methyl derivatives to outperform the ethyl derivatives at both 80 and 100 $^{\circ}$C, a trend that has been seen previously,[19]; the opposite trend has also been reported.[6z] Within the series **1** - **6**, on changing the sterics of the precursor aniline, there is little change in the conversion rates for either the methylaluminium or ethylaluminium derivatives.

Typically, on increasing the temperature, the conversion rates increase, e.g. Figure S6 (SI) for complex **5**. In the case of the systems derived from 1-NH_2,2-$PPh_2C_6H_4$ (**8** and **9**), use of complex **9** appears to be more efficient and more controlled (narrower PDI). Similar trends are observed for those systems derived from diphenylaniline with complex **10** outperforming the systems bearing the phenoxyimine motif. However, it should be noted that isolated polymer yields were moderate to good, for example for run 21 (table 1) using **8**, the yield was 36 %. Again, these systems produced polymers with lower molecular weight than the calculated M_n values, particularly at lower temperatures. The much lower observed molecular weight obtained in some cases is suggestive of either the presence water acting as a chain transfer agent and/or side reactions.

When conducting the polymerizations in the absence of solvent (Table S5, SI), the observed molecular weights were in general much closer to the calculated M_n values, and at 80 °C for 13 mins or less, all complexes achieved excellent conversions (> 97%) with varying degrees of control (PDIs 1.28 – 3.55).

^{1}H and ^{13}C NMR spectra of selected polymers (Table 1, entries 4 and 11) were obtained in order to verify the molecular weights and to identify the end groups present (see Figs. S7 and S8, SI). For entries using pre-catalyst **3** (and **5**), peaks at δ 7.33 ppm ($C_6H_5CH_2$-), 5.27 ppm ($C_6H_5CH_2$-), and 3.62 ppm (CH_2CH_2OH) with an integral ratio of 5:2:2 indicated that the polymers were capped by a benzyl alkoxy group and a hydroxyl end group. ^{13}C NMR data also revealed peaks at δ 127.52 ppm ($C_6H_5CH_2$-), 69.21 ppm ($C_6H_5CH_2$-) and 64.24 ppm (CH_2CH_2OH). The MALDI-ToF spectrum of the PCL (see Fig. S9, SI) revealed the presence of a benzyloxy initiating group and a series of peaks separated by 114.14 mass units (the molecular weight of the monomer). A 'blank run' conducted under the same conditions but using only trimethylaluminium and BnOH (i.e. no dpg or benz-derived ligands were present) failed to afford any polymer (see Table S6, SI).

Table 1. ROP of ε-caprolactone using complexes **1 – 11** (not **2**). Insert here (reviewers, please see end of paper).

A kinetic study of the ε-CL polymerization using **1, 5, 9** and **10** (see Figs. 7 and 8) was undertaken by removing 0.3 ml from the reaction mixture and analyzing by ^{1}H NMR spectroscopy at the appropriate time under the conditions[CL]:[**Cat**]:[BnOH] = [250]:[1]:[1] at 80 °C in toluene. The polymerization rate of the ROP of ε-CL exhibited a first order dependence on the ε-CL concentration (Fig. 8, left) and that the ε-CL conversion reached >95 % over 80 min (Fig. 8, right). From Fig. 8, the rate order **1** > **5** > **9** > **10** was observed suggesting that the presence of the phenoxy (salicylaldimine) motif may well be beneficial, although this is only a tentative suggestion given the differing structures of the complexes. Indeed, it could be argued that the presence of the multiple metal centres in **9** and **10** is detrimental to the rate. The data here (and that for the ROP of *rac*-LA) also suggested that these catalysts require an induction period, suggestive of slow activation.
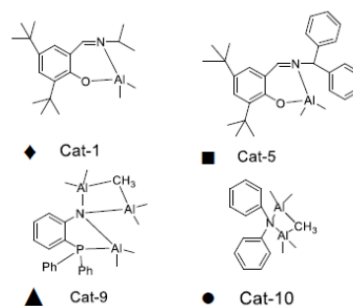
Figure 7. Complexes used in the kinetic study.
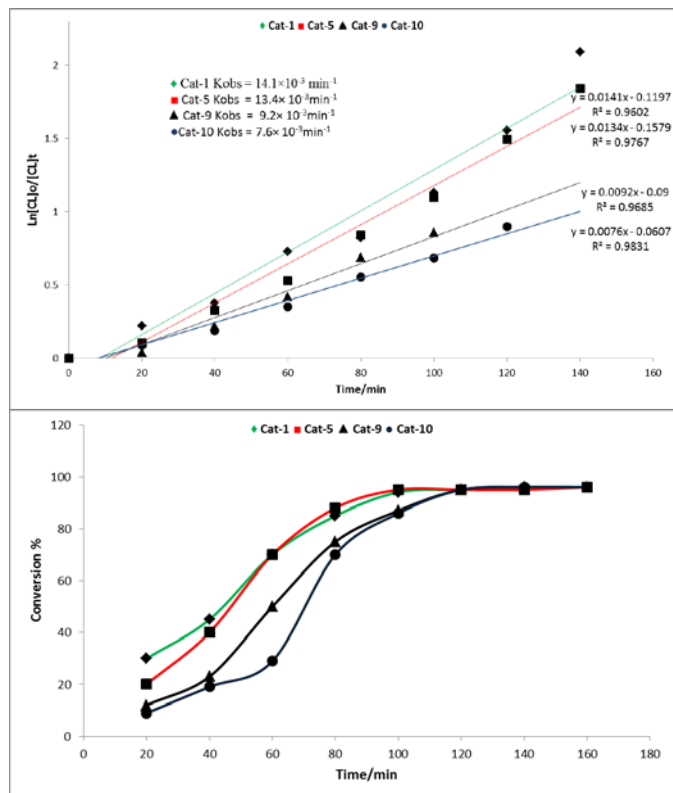
Figure 8. Left: Plot of $\ln[CL]_o/[CL]_t$ *vs* time using complex **1, 5, 9** and **10**; Right : Relationship between conversion and time for the polymerization of CL using complex **1, 5, 9** and **10**.

Ring Opening Polymerization (ROP) of *rac*-Lactide (*rac*-LA)

Scheme 5. ROP of *rac*-LA

The ROP of *rac*-Lactide (*rac*-LA) was conducted using **1** - **11** in the presence of BnOH (scheme 5). All complexes were active, and the polymerizations were mostly well controlled (PDIs 1.04 – 2.36; only 3 runs gave PDIs > 1.5), although conversions were somewhat lower than those observed for ε-CL. Indeed, in most cases, it proved necessary to conduct the polymerizations over 12 h to achieve reasonable conversion. Increasing the molar ratio of *rac*-LA to [Al] did not drastically influence the conversion rates

but appeared, in general, to increase the polymer molecular weight (M_n); increasing the polymerization time tended to have the same effect. The relationship between M_n and PDI of the polymer and the mole ratio [*rac*-LA]/[BnOH] for **3** (Table 2 entries 4-8) is displayed in Fig. S10 (SI), and reveals a saturation curve for the former. In the case of the PDI, the relationship with [*rac*-LA]/[BnOH] suggests that transesterification might be an issue at high monomer loadings leading to molecular weight suppression.

For **3** (Table 2 entries 4-8) the relationship between monomer conversions and M_n values (Fig. S11, SI) is exponential.

^{1}H and ^{13}C NMR spectra of selected polymers (Table 2, entries 3 and 14) were obtained in order to verify the molecular weights and to identify the end groups present (see Figs. S12 and S13, SI). For entries using pre-catalyst **5** and **6**), peaks at δ 7.12, 5.11, and 3.60 ppm (5:2:2) indicated that the polymers were capped by a benzyl alkoxy group and a hydroxyl end group. ^{13}C NMR data also revealed peaks at δ 127.63 ($C_6H_5CH_2$-), 69.06 ($C_6H_5CH_2$-) and 63.99 ppm (CH_2CH_2OH). The MALDI TOF spectrum of the PLA (Figs. S14 and S15, SI; runs 17 and 23, Table 2) revealed the presence of a benzyloxy initiating group and a series of peaks separated by the mass of one lactide unit (72.0).

A kinetic study of the *rac*-LA polymerization using **1**, **5**, **9** and **10** was undertaken by removing 0.3 ml from the reaction mixture and analyzing by ^{1}H NMR spectroscopy at the appropriate time under the conditions [*rac*-LA]:[**Cat**]:[BnOH] = [100]:[1]:[1] at 110 °C in toluene. The polymerization rate of the ROP of *rac*-LA exhibited a first order dependence on

the *rac*-LA concentration (Fig. 9, left) and that the *rac*-LA conversion reached >70% over 12 h. (Fig 9, right). The same order of reactivity was observed here as for the ε-CL case, although for **1** and **5** there was a clear rate enhancement after 6 and 8 h respectively.
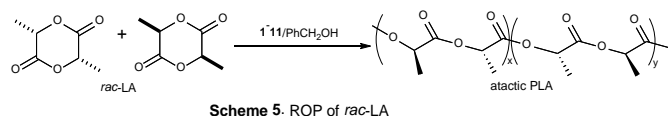
Table 2. ROP of *rac*-Lactide (*rac*-LA) using complexes **1**-**11**. Insert here (reviewers, please see end of paper).
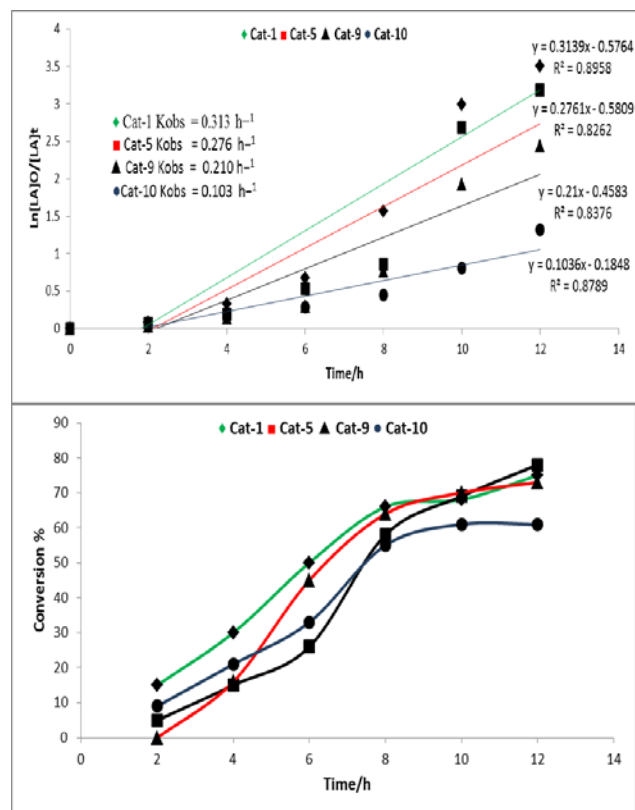
Figure 9. Left: Plot of $\ln[rac\text{-LA}]_o/[rac\text{-LA}]_t$ *vs* time using **1**, **5**, **9** and **10**; Right: Relationship between

conversion and time of polymerization *rac*-LA using **1**, **5**, **9** and **10**.

To assign the stereochemistry of the PLA polymers, we employed 2D *J*-resolved and homonuclear decoupled ^{1}H NMR spectroscopy, and assigned peaks by reference to the literature.[20] Representative spectra for runs 21 and 26 are given in the SI (Figs. S16 – S19), with the assignments given on the respective figures; these systems gave atactic PLA as reported elsewhere for this observed spectral pattern.[21]

Of the complexes displayed in Chart S1 (SI), pre-catalysts **III**, **V**, **X** and **XXVII** closely resemble structures **1** - **8** herein. System **3** bearing an imine-bound pentafluorophenyl group and only one (*ortho*) *tert*-butyl substituent on the phenoxy moiety is more active at lower temperatures over shorter reaction times affording higher molecular weight products, particularly in the case of ε-CL and δ-VL.[6c] Pre-catalyst **V**, bearing a 2,4-difluorophenyl group at N, is a little slower than **III** for the ROP of ε-CL and is comparable with **1** – **8** herein, although the polymer molecular weight is somewhat reduced *cf* **III**, it is still higher than observed for the PCL herein.[6e] System **X**, possessing a *para* isopropyl substituent on the N bound aryl but bearing 3, 5-di-*tert*-butyl groups on the phenoxy as for **1** – **8** herein, has comparable activity for the ROP of *rac*-LA requiring 48 h to achieve complete conversion but affords higher molecular weight PLA.[6i] Pre-catalysts **XXVII** possess an N bound CHPh$_2$, but with no *tert*-butyl substituents on the phenoxy (or thiophenoxy) motif,[6z] and these Me$_2$Al systems can most closely

be compared with **5**. For ε-CL, results using **5** (run 9, Table 1) at ambient temperature are similar to those of the phenoxy version of **XXVII** (M_{nGPC} = 3100, PDI, 89 %) albeit under slightly different conditions (ROP of **XXVII** employed a ratio of 100:1:2 [ε-CL]:[Al]:[OH] over 6 h). For the ROP of *L*-LA, **XXVII** required a higher temperature than for ε-CL (as observed herein) and afforded PLA with M_{nGPC} in the 5000 – 6000 region.

Co-polymerization of ε-Caprolactone and *rac*-Lactide (*rac*-LA)

Complexes **1** - **11** have also been screened for their potential to act as catalysts for the co-polymerization of ε-CL with *rac*-LA under the optimum conditions found for the homo-polymerizations in toluene, i.e. at 80°C for 1 h with ε-CL followed by stirring for 12 h at 110 °C with *rac*-LA. In all cases (Table 3), good yields (54 - 88%) of co-polymer were formed, and with appreciable lactide content (35 to 62.6%) as observed by ^{1}H NMR spectra (Fig. S20, SI); both ^{1}H and ^{13}C NMR spectra (Fig. S21, SI) were assigned as per the literature.[22] The highest % incorporation of LA was found for **1** (62.6%). Observed molecular weights (3680 - 6670) are best described as low to moderate, however we note there is interest in low molecular weight poly(lactide/caprolactone) polymers as bio-adhesives.[23] Thermal analysis of the co-polymers by DSC revealed two melting points at 55.7 °C (PCL) and 125.9 °C (PLA), see Fig. S22, SI.

Table 3. Synthesis of diblock co-polymers from cyclic ester monomers (ε-CL+ *rac*-LA).

Run[a]	Cat	CL:LA[b]	Yield	M_n[c]	PDI[d]
1	**1**	37.5:62.5	70	4850	1.31
2	**2**	38.5:61.5	77	5000	1.23
3	**3**	45:55	54	6670	1.43
4	**4**	44.5:55.5	80	6500	1.26
5	**5**	59:41	62	4620	1.29
6	**6**	57.5:42.5	56	4650	1.22
7	**7**	57:43	88	5840	1.34
8	**8**	65:35	55	3680	1.66
9	**9**	55.5:44.5	70	6000	1.23
10	**10**	43.5:56.5	60	5500	1.48
11	**11**	42.5:57.5	65	5770	1.41

[a] Optimum conditions: 1h ε-CL 80 °C/12h *rac*-LA 110 °C, (100 ε-CL: 100 *rac*-LA: 1 BnOH). [b] Ratio of LA to CL observed in the co-polymer by ^{1}H NMR. [c] M_n values were determined by GPC in THF *vs* PS standards and were corrected with a Mark–Houwink factor ($M_{n,\ GPC}$ × 0.56 × % PCL + $M_{n,GPC}$ × 0.58 × % P *rac*-LA). [d] PDI were determined by GPC.

Ring Opening Polymerization (ROP) of δ-valerolactone
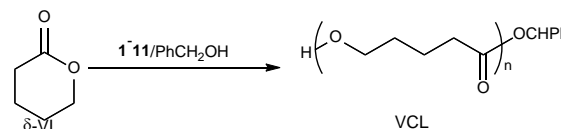
Scheme 6. ROP of δ-VL

For the δ-VL ROP reactions (Table 4, scheme 6), 110 °C over 12 h was generally required to achieve reasonable conversion, and the resulting ROP reactions were all well-behaved with PDIs in the range 1.10 - 1.73. The relationship between M_n and PDI of the PVL and the mole ratio [VL]/[BnOH] for **5** (Table 4 entries 7-10) are near linear (Fig. S23, SI). In general, the ROP of δ-VL was slower than that of ε-CL, which is consistent with the thermodynamic parameters for these lactones.[24] Within the series **1** - **6**, %conversions increased on increasing bulk of the aniline derived moiety. In the case of **7** and **8**, the presence of either the amine linkage or phosphine function respectively, appeared to be detrimental to the activity. The non-Schiff-base systems **9** - **11** required longer (24 h) to achieve reasonable %conversion. Molecular weights (M_n) for all systems were somewhat lower than calculated values. [1]H

NMR spectra of the resultant polymers (e.g. Fig. S2**4**, SI) indicated the presence of benzyloxy and OH end groups. As mentioned previously, comparison with the systems in Table S1 for the ROP of δ-VL reveals that they are inferior to the phenoxyimine system **III** bearing a C_6F_5 group at the imino N which operates under milder conditions and affords far higher molecular weight products, but are comparable with the performance of system **VI**.[6c, 6f]

Table 4. ROP of δ-valerolactone using Al complex **1-11** Insert here (reviewers, please see end of paper).

Conclusion

In conclusion, we have prepared and structurally characterized a number of organoaluminium phenoximine complexes and have also investigated the structures of the complexes resulting from reaction of the precursor anilines with organoaluminium reagents, i.e. minus the salicylaldimine motif. In the presence of benzyl alcohol the complexes were active for the ROP of ε-caprolactone, δ-valerolactone and *rac*-lactide and were also capable of the co-polymerization of ε-caprolactone/*rac*-lactide with reasonable (up to 62.6%) lactide incorporation. In the case of the ROP of ε-CL and *rac*-LA, there was indication of catalytic misbehaviour with non-linear plots and slightly broad (c.a. 2.0) PDIs. The systems bearing the salicylaldimine motif exhibited increased rates for these ROP studies. However, given that those complexes which did not possess this motif had more than one metal centre present, we can only tentatively propose that the presence of the salicylaldimine (phenoxy) motif is beneficial in the systems studied

herein. In the case of δ-valerolactone, shorter polymerization times were possible for the Schiff-base systems.

Experimental

General:

All manipulations were carried out under an atmosphere of dry nitrogen using conventional Schlenk and cannula techniques or in a conventional nitrogen-filled glove box. Hexane and Toluene was refluxed over sodium. Acetonitrile was refluxed over calcium hydride. All solvents were distilled and degassed prior to use. IR spectra (nujol mulls, KBr windows) were recorded on a Nicolet Avatar 360 FT IR spectrometer; ^{1}H NMR spectra were recorded at room temperature on a Varian VXR 400 S spectrometer at 400 MHz or a Gemini 300 NMR spectrometer or a Bruker Advance DPX-300 spectrometer at 300 MHz. The ^{1}H NMR spectra were calibrated against the residual protio impurity of the deuterated solvent. Elemental analyses were performed by the elemental analysis service at the London Metropolitan University and in the Department of Chemistry, the University of Hull. The precursor $1-NH_2,2-PPh_2C_6H_4$ was prepared by the literature method.[25] The pro-ligands L^1H and L^4H, and the complexes **1** and **7** were prepared as described previously.[10, 11]

Synthesis of $Ph,MeCHN=CH(3,5-tBu_2C_6H_2-OH-2)$ **L²H**

To a solution of 3,5-di-*tert*-butylsalicylaldehyde (2.34 g, 10.0 mmol) with a few drops of glacial acetic acid in anhydrous ethanol (15 ml) under argon at 50

°C was added a solution of α-methylbenzylamine (1.21 g, 10.0 mmol) in anhydrous ethanol (15 ml) over a period of 30 min with stirring. The mixture was then refluxed for an additional 6 h. Upon cooling to ambient temperature, the volatiles were removed under vacuo, and the residue was recrystallized from ethanol at −20 °C to give **L²**H as a yellow powder. Yield 3.2 g, 95%. Elemental analysis calculated for $C_{23}H_{31}NO$: C, 81.85; H, 9.26; N, 4.15. Found: C, 81.67; H, 9.33; N, 4.27%. IR (nujol null, KBr): 3441 (m), 2967 (s), 2868 (m), 2358 (w), 1626 (s), 1585 (w), 1464 (w), 1452 (w), 1438 (w), 1383 (m), 1360 (m), 1343 (w), 1322 (w), 1270 (m), 1248 (s), 1207 (m), 1174 (s), 1135 (w), 1115 (w), 1075 (m), 1029 (w), 976 (m), 906 (w), 880 (w), 824 (m), 773 (m), 759 (s), 730 (w), 700 (s), 644 (w), 631 (w), 594 (w), 541 (m), 499 (w). MS (ESI, positive mode): 338.4 MH⁺. ¹H NMR (400 MHz, CDCl₃): δ 13.68 (s, 1 H, O*H*), 8.43 (s, 1 H, C*H*=N), 7.40 - 7.33 (m, 5 H, Ar-*H*), 7.28 - 7.26 (m, 1 H, Ar-*H*), 7.86 (d, *J* = 2.4 Hz, 1 H, Ar-*H*), 4.56 - 4.52 (m, 1 H, C*H*(CH₃)), 1.65 (d, *J* = 6.4 Hz, 3 H, CH(C*H*₃)), 1.46 (s, 9 H, C(C*H*₃)₃), 1.30 (s, 9 H, C(C*H*₃)₃).

Synthesis of Ph₂CHN=CH(3,5-*t*Bu₂C₆H₂-OH-2) **L³**H

By using the procedure described above for synthesis of **L²**H, the ligand **L³**H was obtained by the reaction of 3,5-di-*tert*-butylsalicylaldehyde (2.34 g, 10.0 mmol) with benzhydrylamine (1.83 g, 10.0 mmol) as a yellow power in 92% yield. Elemental analysis calculated for $C_{28}H_{33}NO$: C, 84.17; H, 8.32; N, 3.51. Found: C, 84.35; H, 8.43; N, 3.47%. IR (nujol mull, KBr, cm⁻¹): 3435 (m), 3060 (w), 3029 (w), 2956 (w), 2868 (w), 2361 (w), 1631 (s), 1586 (w), 1493 (w), 1455 (m), 1386 (m), 1357 (m), 1342 (w), 1322 (w), 1269 (m), 1246 (s), 1204 (m), 1171 (s), 1133 (w), 1089 (m), 1050 (s), 1028 (s), 980 (w), 916 (w), 880 (w), 846 (w), 827 (m), 800 (w), 766 (m), 746 (m), 733 (w), 703 (s), 644 (w), 620 (w), 612 (w), 561 (w), 538 (w), 509 (w), 468 (w). MS (ESI, positive mode): 400.2 MH⁺. ¹H NMR (400 MHz, CDCl₃) δ: 13.74 (s, 1 H, O*H*), 8.41 (s, 1 H, C*H*=N), 7.32 (d, *J* = 2.4 Hz, 1 H, Ar-*H*), 7.28 - 7.23 (m, 8 H, Ar-*H*), 7.19 - 7.15 (m, 2 H, Ar-*H*), 7.01 (d, *J* = 2.4 Hz, 1 H, Ar-*H*), 5.52 (s, 1 H, C*H*(Ph)₂), 1.38 (s, 9 H, C(C*H*₃)₃), 1.21 (s, 9 H, C(C*H*₃)₃).

Synthesis of Ph₂CHN=CH₂(3,5-*t*Bu₂C₆H₂-OH-2) **L³**H via dpg

2,2′-Diphenylglycine (1.13 g, 5.00 mmol) and 2-hydroxy-3,5-di-*tert*-butylsalicylaldehyde (1.17 g, 5.00 mmol) were refluxed in ethanol for 3 days using a Dean-Stark condenser. Following removal of the ethanol, the residue was triturated with methanol (50 ml), filtered and dried. Yield: 1.26 g, 63%. $C_{28}H_{33}NO·⅔MeOH$ requires C 81.82, H 8.54, N 3.33 %. Found: C 81.96, H 8.65, N 3.34%. IR (nujol mull, KBr, cm⁻¹): 3432 (bs), 1629 (s), 1603 (m), 1577 (w), 1477 (s), 1446 (s), 1393 (m), 1361 (m), 1297 (w), 1260 (s), 1236 (m), 1203 (m), 1163 (m), 1078 (w), 1025 (m), 947 (w), 875 (m), 780 (w), 758 (m), 726 (w), 686 (s), 672 (w), 646 (w), 592 (w), 539 (w), 454 (w). MS (ES, positive mode): 400.4 MH⁺. ¹H NMR (400 MHz, CDCl₃) δ: 13.84 (s, 1 H, O*H*), 8.52 (s, 1 H, C*H*=N), 7.42 (d, *J* = 2.4 Hz, 1 H, Ar-*H*), 7.37 - 7.34 (m, 8 H, Ar-*H*), 7.29 - 7.26 (m, 2 H, Ar-*H*), 7.26 (d, *J* = 2.4 Hz, 1 H, Ar-*H*), 5.63 (s, 1 H, C*H*(Ph)₂), 1.49 (s, 9 H, C(C*H*₃)₃), 1.32 (s, 9 H, C(C*H*₃)₃).

Synthesis of [*i*PrCHN=CH(3,5-*t*Bu$_2$C$_6$H$_2$-O-2)AlEt$_2$] (**2**)

A solution of AlEt$_3$ (1.9 ml, 3.0 mmol, 2 M in toluene) was added at room temperature to a solution of *i*PrCHN=CH(3,5-*t*Bu$_2$C$_6$H$_2$-OH-2) **L^{1}H** (0.74 g, 2.7 mmol) in toluene (25 mL) over a period of 30 min with stirring. Then the mixture was refluxed for an additional 12 h. Upon cooling to room temperature, the volatiles were removed under vacuo, and the residue was recrystallized from acetonitrile to give **2** as a yellow solid. Yield 0.53 g, 55%. Elemental analysis calculated for C$_{22}$H$_{38}$AlNO: C, 73.50; H, 10.65; N, 3.90. Found: C, 73.33; H, 10.35; N, 3.73%. IR (nujol mull, KBr, cm^{-1}): 3730 (w), 2959 (s), 2871 (m), 1629 (s), 1553 (m), 1470 (m), 1445 (m), 1422 (m), 1385 (m), 1361 (m), 1318 (w), 1276 (m), 1258 (m), 1238 (w), 1203 (w), 1179 (m), 1163 (w), 1118 (s), 1058 (w), 1025 (w), 977 (w), 955 (w), 855 (m), 785 (m), 754 (w), 716 (w), 647 (w), 526 (w), 411 (w). MS (ES, positive mode): 359.2 M. ^{1}H NMR (400 MHz, CDCl$_3$): δ: 8.12 (s, 1 H, C*H*=N), 7.42 (d, *J* = 2.0 Hz, 1 H, Ar-*H*), 6.90 (d, *J* = 2.0 Hz, 1 H, Ar-*H*), 3.72 - 3.65 (m, 1 H, C*H*(CH$_3$)$_2$), 1.37 (d, *J* = 3.2 Hz, 6 H, -CH(C*H$_3$*)$_2$), 1.34 (s, 9 H, -C(C*H$_3$*)$_3$), 1.21 (s, 9 H, C(C*H$_3$*)$_3$), 0.94 - 0.90 (m, 6 H, Al(CH$_2$C*H$_3$*)$_2$), –0.07 - (–0.22) (m, 4 H, Al(C*H$_2$*CH$_3$)$_2$).

Synthesis of [Me,PhCHN=CH(3,5-*t*-Bu$_2$C$_6$H$_2$-O-2)AlMe$_2$] (**3**)

A solution of AlMe$_3$ (1.6 mL, 2.50 mmol, in toluene 1.6 M) was added at room temperature to a solution of Ph,MeCHN=CH(3,5-*t*Bu$_2$C$_6$H$_2$-OH-2) **L^{2}H** (0.77 g 2.30 mmol) in hexane (25 mL). The resulting yellow solution was stirred for 12 h. The solution was

filtered and concentrated, affording **3** a yellow solid. Yield 0.60 g, 67%. Elemental analysis calculated for C$_{25}$H$_{36}$AlNO: C, 76.30; H, 9.22; N, 3.56. Found: C, 76.25; H, 9.31; N, 3.40%. IR (nujol mull, KBr, cm^{-1}): 3429 (s), 3064 (w), 3037 (w), 2960 (s), 2866 (m), 2358 (w), 2335 (w), 1616 (s), 1553 (m), 1543 (m), 1469 (m), 1454 (m), 1439 (m), 1414 (m), 1391 (m), 1355 (m), 1322 (s), 1299 (w), 1275 (w), 1254 (s), 1237 (w), 1200 (m), 1178 (s), 1138 (w), 1085 (m), 1058 (w), 1029 (w), 990 (w), 932 (w), 910 (w), 880 (w), 855 (s), 816 (w), 782 (m), 763 (s), 702 (s), 674 (s), 613 (w), 596 (w), 537 (m), 490 (w), 410 (w). MS (ESI): $^m/_z$ 378.6 [M – Me] $^+$, 363.6 [M – 2Me]$^+$. ^{1}H NMR (400 MHz, CDCl$_3$) δ: 8.11 (s, 1 H, C*H*=N), 7.49 - 7.36 (m, 5 H, Ar-*H*), 7.18 (s, 1 H, Ar-*H*), 6.90 (s, 1 H, Ar-*H*), 4.93 - 4.92 (m, 1 H, C*H*(CH$_3$)), 1.78 - 1.76 (d, *J* = 4.0 Hz, 3 H, CH(C*H$_3$*)), 1.39 (s, 9 H, C(C*H$_3$*)$_3$), 1.27 (s, 9 H, C(C*H$_3$*)$_3$), –0.79 (s, 3 H, AlC*H$_3$*), –0.93 (s, 3 H, AlC*H$_3$*).

Synthesis of [Me,PhCHN=CH(3,5-*t*Bu$_2$C$_6$H$_2$-O-2)AlEt$_2$] (**4**)

As for **2**, but using Me,PhCHN=CH(3,5-*t*Bu$_2$C$_6$H$_2$-OH-2) **L^{2}H** (0.77 g, 2.30 mmol) and AlEt$_3$ (1.6 ml, 2.50 mmol, 1.6 M in toluene) affording **4** as a yellow solid. Yield 0.6 g, 62%. Elemental analysis calculated for C$_{27}$H$_{40}$AlNO: C, 76.92; H, 9.56; N, 3.32. Found: C, 76.65; H, 9.33; N, 3.28%. IR (nujol mull, KBr, cm^{-1}): 3423 (w), 2954 (s), 2866 (w), 1627 (s), 1559 (m), 1473 (m), 1444 (w), 1422 (m), 1388 (w), 1361 (w), 1277 (m), 1258 (m), 1236 (w), 1202 (m), 1176 (s), 1134 (w), 1120 (w), 1081 (w), 1056 (w), 1034 (w), 982 (w), 910 (w), 874 (w), 852 (m), 787 (w), 758 (m), 715 (w), 699 (w), 605 (w), 524 (w). MS (ESI): $^m/_z$ 392 [M – Et] $^+$, 363 [M – 2Et] $^+$. ^{1}H NMR

(400 MHz, CDCl$_3$) δ: 8.12 (s, 1 H, CH=N), 7.49 (d, J = 2.0 Hz, 1 H, Ar-H), 7.42-7.34 (s, 5 H, Ar-H), 6.88 (d, J = 2.0 Hz, 1 H, Ar-H), 4.56 - 4.51 (m, 1 H, CH(CH$_3$)), 1.78 (d, J = 7.0 Hz, 3 H, CH(CH_3)), 1.40 (s, 9 H, CH(CH_3)), 1.26 (s, 9 H, CH(CH_3)), 0.97 - 0.85 (m, 6 H, Al(CH$_2$CH_3)$_2$), –0.72 - (–0.31) (m, 4 H, Al(CH_2CH$_3$)$_2$).

Synthesis of [Ph$_2$CHN=CH(3,5-tBu$_2$C$_6$H$_2$-O-2)AlMe$_2$] (**5**)

As for **2**, but using Ph$_2$CHN=CH(3,5-tBu$_2$C$_6$H$_2$-OH-2) **L^{3}H** (1.00 g, 2.50 mmol) and AlMe$_3$ (1.70 mL, 2.70 mmol, in toluene 1.6 M) afforded **3** as yellow crystals. Single crystals suitable for X-ray analysis were grown from a saturated hexane solution. The solution was filtered and concentrated, affording **5** as a yellow crystalline solid. Yield 0.90 g, 79%. Elemental analysis calculated for C$_{30}$H$_{38}$AlNO: C, 79.09; H, 8.41; N, 3.07. Found: C, 79.19; H, 8.28; N, 3.20%. IR (nujol mull, KBr, cm^{-1}): 3428 (w), 2965 (s), 2866 (w), 1616 (s), 1561 (w), 1543 (s), 1469 (s), 1441 (m), 1424 (s), 1389 (m), 1362 (m), 1344 (w), 1318 (s), 1275 (w), 1258 (s),1241 (w), 1199 (w), 1183 (s), 1164 (m), 1148 (m), 1134 (m), 1026 (w), 995 (m), 965 (w), 924 (w), 887 (m), 855 (s), 807 (w), 784 (m), 760 (s), 708 (w), 677 (s), 641 (w), 602 (m), 552 (m), 491 (m), 410 (w). MS (ESI): $^m/_z$ 423.6 [M - 2Me]$^+$. ^{1}H NMR (400 MHz, CDCl$_3$) δ: 8.00 (s, 1 H, CH=N), 7.52 (d, J = 2.6 Hz, 1 H, Ar-H), 7.42 - 7.32 (m, 6 H, Ar-H), 7.23 - 7.18 (m, 4 H, Ar-H), 6.81 (d, J = 2.5 Hz, 1 H, Ar-H), 6.23 (s, 1 H, CHPh$_2$), 1.40 (s, 9 H, C(CH_3)$_3$), 1.26 (s, 9 H, C(CH_3)$_3$), –0.96 (s, 3 H, AlCH_3), –0.97 (s, 3 H, AlCH_3). For [Ph$_2$CHNCH$_2$(3,5-tBu$_2$C$_6$H$_2$-OH-2)AlMe$_2$] (**7**): Yield *ca*. 10 %. ^{1}H NMR (C$_6$D$_6$, 400 MHz) δ: 7.31 -

6.40 (6× m, 12H, Ar-H), 4.09 (s, 2H, CH_2), 1.42 (s, 9 H, C(CH_3)$_3$), 1.13 (s, 9 H, C(CH_3)$_3$), –0.97 (s, 6 H, AlCH_3). ^{13}C NMR (C$_6$D$_6$): –10.01 (AlCH_3).

Synthesis of [Ph$_2$CHN=CH(3,5-tBu$_2$C$_6$H$_2$-O-2)AlEt$_2$] (**6**)

As for **5**, but using Ph$_2$CHN=CH(3,5-tBu$_2$C$_6$H$_2$-OH-2) **L^{3}H** (1.00 g, 2.50 mmol) and AlEt$_3$ (1.35 ml, 2.75 mmol, 2.0 M in toluene) affording **7** as a yellow solid. Yield 0.76 g, 63%. Elemental analysis calculated for C$_{32}$H$_{42}$AlNO: C, 79.46; H, 8.75; N, 2.90. Found: C, 79.25; H, 8.33; N, 2.67%. IR (nujol mull, KBr, cm^{-1}): 3694 (w), 3428 (w), 2954 (s), 2855 (w), 1616 (s), 1556 (w), 1543 (m), 1493 (w), 1463 (w), 1417 (w), 1392 (m), 1359 (w), 1329 (w), 1280 (w), 1254 (w), 1232 (w), 1198 (w), 1174 (m), 1004 (m), 988 (w), 916 (w), 879 (w), 852 (w), 784 (w), 757 (w), 730 (w), 699 (s), 640 (m), 538 (w). MS calculated for **7** ($^m/_z$): 483.31 (100.0%), 484.31 (35.5%), 485.31 (6.1%). Found MS (ESI): $^m/_z$ 423.7 [M – Et]$^+$. ^{1}H NMR (400 MHz, CDCl$_3$) δ: 7.99 (s, 1 H, CH=N), 7.51 (d, J = 2.8 Hz, 1 H, Ar-H), 7.39 - 7.35 (m, 6 H, Ar-H), 7.22 - 7.20 (m, 4 H, Ar-H), 6.78 (d, J = 2.8 Hz, 1 H, Ar-H), 6.20 (s, 1 H, CHPh$_2$), 1.41 (s, 9 H, C(CH_3)$_3$), 1.25 (s, 9 H, C(CH_3)$_3$), 0.87 - 0.83 (m, 6H, Al(CH$_2$CH_3)$_2$), –0.23 - –0.36 (m, 4 H, Al(CH_2CH$_3$)$_2$).

Synthesis of {Ph$_2$PC$_6$H$_4$N[(Me$_2$Al)$_2$μ-CH$_3$](μ-Me$_2$Al)} (**9**)

To 1-NH$_2$,2-PPh$_2$C$_6$H$_4$ (1.50 g, 5.41 mmol) in toluene (20 ml) was added Me$_3$Al (5.41 ml, 2.0 M, 10.8 mmol) and the system was refluxed for 12 h. On cooling, the volatiles were removed *in vacuo*, and the residue was extracted into warm MeCN (20 ml).

Prolonged standing (2 - 3 days) at ambient temperature afforded small white prisms of **9**. Yield 1.12 g, 56%. Elemental analysis calculated for $C_{25}H_{35}Al_3NP \cdot 0.87MeCN \cdot 0.39toluene$: C, 66.43; H, 7.64; N, 4.2 %. Found: C, 66.39; H, 7.64; N, 4.92%. IR (nujol mull, KBr, cm^{-1}): 2940 (m), 2923 (s), 2853 (s), 2725 (w), 2671 (w), 1610 (m), 1586 (w), 1457 (s), 1377 (s), 1301 (m), 1260 (m), 1182 (w), 1157 (w), 1089 (m), 1068 (m), 1026 (m), 891 (w), 801 (m), 743 (m), 722 (m), 695 (s), 548 (w), 505 (w), 492 (w), 474 (w). MS (ES, positive mode): $^m/_z$ 389 [M – Al(CH$_3$)$_3$]. ^{1}H NMR (CDCl$_3$) δ: 7.36 - 7.34 (m, 2H, C$_6$*H*$_2$), 7.32-7.28 (m, 10H, *Ph*P), 6.78–6.66 (m, 2H, C$_6$*H*$_2$), 2.33(s, H, *toluene*), 2.26 (bs, 3H, Al-*CH$_3$*-Al), 2.00(s,3H, *MeCN* –0.81(bs, 18H, *CH$_3$*-Al). ^{31}P NMR (CDCl$_3$) δ: –19.80.

Synthesis of {Ph$_2$N[(Me$_2$Al)$_2$ μ-Me]} (**10**)

To Ph$_2$NH (0.84 g, 5.0 mmol) in toluene (30 ml) was added Me$_3$Al (5.0 ml, 2.0 M, 10.0 mmol), and the system was refluxed for 12 h. On cooling, the volatiles were removed *in-vacuo*, and the residue was extracted into warm acetonitrile (30 ml). Cooling to 0 °C afforded colourless prisms of **10**: 0.92 g, 62.5%. X-ray quality crystals were obtained from MeCN. $C_{17}H_{25}Al_2N \cdot \frac{1}{3}MeCN$ requires C 68.22, H 8.35, N 5.98 %. Found: C 68.76, H 8.35, N 6.00%. IR (nujol mull, cm^{-1}): 3414 (w), 3192 (w), 2953 (s), 2922 (s), 2852 (s), 2727 (w), 2670 (w), 1936 (w), 1876 (w), 1788 (w), 1594 (s), 1520 (s), 1493 (s), 1415 (s), 1376 (s), 1339 (w), 1310 (m), 1261 (m), 1201 (s), 1079 (s), 1029 (s), 1005 (w), 917 (m), 846 (s), 801 (s), 746 (m), 694 (s), 608 (m), 570 (m), 524 (m), 503 (m), 482 (w), 479 (m). MS (ES, positive mode): 225.6 M$^+$ –Al(CH$_3$)$_3$. ^{1}H NMR (400 MHz, CD$_3$CN) δ: 7.17 -

6.77 (m, 10H, Ar-*H*), 2.17 (s, 1H, N-*H*), 1.94 (s, 3H, Al-*CH$_3$*-Al), –0.87 (s, 6H, Al*CH$_3$*), –0.96 (s, 6H, Al*CH$_3$*).

Synthesis of [Ph$_2$CHNH(μ-Me$_2$Al)]$_2$·MeCN (**11·MeCN**)

As for **9**, but using Ph$_2$CHNH$_2$ (0.91 g, 5.0 mmol) and Me$_3$Al (2.5 ml, 2.0 M, 5.0 mmol) affording **10** as colourless needles. Yield 1.12 g, 47.2%. $C_{30}H_{36}Al_2N_2$ requires C 75.29, H 7.58, N 5.89%. Found: C 74.68, H 8.20, N 5.72 %. IR (nujol mull, KBr, cm^{-1}): 3286 (m), 2925 (s), 2857 (s), 2726 (w), 2672 (w), 1967 (w), 1946 (w), 1799 (w), 1622 (m), 1539 (w), 1494 (s), 1453 (s), 1377 (s), 1316 (m), 1259 (m), 1187 (s), 1080 (s), 1039 (s), 1017 (s), 916 (m), 874 (s), 819 (s), 758 (m), 742 (m), 697 (s), 594 (m), 570 (m), 509 (m), 499 (m), 479 (m), 451 (w). MS (ES, positive mode): MH$^+$ 479, [MH$^+$ + MeCN] 519. ^{1}H NMR (400 MHz, CDCl$_3$) δ: 7.40 - 7.15 (m, 20H, Ar-*H*), 5.10 (s, 1H, C*H*(Ph)$_2$), 5.07(s, 1H, C*H*(Ph)$_2$), 2.17 (s, 1H, N-*H*), 2.14 (s, 1H, N-*H*), 1.98 (s,3H, *Me*CN), –0.97(s, 6H, Al*CH$_3$*), –1.02(s, 6H, Al*CH$_3$*).

Ring opening polymerization.

Typical polymerization procedures in the presence of one equivalent of benzyl alcohol (Table 4, run 1) are as follows. A toluene solution of **3** (0.010 mmol, 1.0 mL toluene) and BnOH (0.010 mmol) were added into a Schlenk tube in the glove-box at room temperature. The solution was stirred for 2 min, and then ε-caprolactone (2.5 mmol) along with 1.5 mL toluene was added to the solution. The reaction mixture was then placed into an oil bath pre-heated to

the required temperature, and the solution was stirred for the prescribed time. The polymerization mixture was then quenched by addition of an excess of glacial acetic acid (0.2 mL) into the solution, and the resultant solution was then poured into methanol (200 mL). The resultant polymer was then collected on filter paper and was dried *in* vacuo.

DSC Procedure

About 2 mg of polymer sample was taken and first heated to the desired temperature 180 ^{o}C then cooled down to a low temperature 25 ^{o}C and heated again to the same temprature. Both heating and cooling rates were (10 ^{o}C/min).

Crystallography

Structures were solved using automated direct methods within SHELXS-86 or intrinsic phasing within SHELXT.[26] Structures were refined by full-matrix least squares refinement within SHELXL-2014 using all unique data.[27, 28] Hydrogen atoms were placed using a riding model. Where data were sufficiently good, methyl group orientations were refined. Many of the structures displayed disorder in the position of methyl groups or in solvent of crystallisation. This disorder was modelled using standard techniques.

Diffraction data were collected on a range of different CCD diffractometers and were corrected for absorption and Lp effects using multi-scan methods.[29] The details are presented in Table 7. For **5** the crystal examined was twinned. The structure was refined using all observed reflections within SHELXL using the HKLF5 formalism. Samples

L^3H(dpa) and L^3H(dpg) were collected at different temperatures from samples made in the same way. In each case the structure determination was repeated using a second crystal to confirm the correctness of the crystal structure at that temperature. Diffraction data for **9** were collected using synchrotron radiation at Daresbury Laboratory Station 9.8. For **10**: The structure was refined as a two-component twin using the HKLF5 protocol as above for **5**. The two domains were related by a 178.8° rotation about the real and direct [010] direction. Two out of three H atoms on CH_3^+ group at C(5) are disordered. In the difference electron density map, one clear peak is seen with a peak height of *ca.* 0.9 eÅ^{-3} which is refined fully occupied as H(5A). There are also *ca.* four smaller peaks of between 0.4-0.6 eÅ^{-3} which are refined in pairs as the other CH_3^+ H atoms. A similar pattern of electron density peaks and partial H-atom disorder was observed in **9**.

CCDC 1480938 - 1480944 contain the supplementary crystallographic data for this paper. These data can be obtained free of charge from The Cambridge Crystallographic Data Centre via www.ccdc.cam.ac.uk/data_request/cif.

of beam time at Daresbury Laboratory and Dr. Simon J. Teat for scientific support.

References

[1] (a) C. K. Williams, *Chem. Soc. Rev*. **2007**, *36*, 1573. (b) A. Arbaoui and C. Redshaw, *Polym. Chem.* **2010**, *1*, 801. (c) W. Alkarekshi, A. P. Armitage, O. Boyron, C. J. Davies, M. Govere, A. Gregory, K. Singh and G. A. Solan, *Organometallics*, **2013**, *32*, 249 and references therein. (d) Y. Liu, W. -S. Dong, J. -Y. Liu and Y. -S. Li, *Dalton Trans.* **2014**, *43*, 2244.

[2] See for example (a) E. Chiellini and R. Solaro, *Adv. Mater.* **1996**, *8*, 305. (b) M. A. Woodruff and D. W. Hutmacher, *Prog. Polym. Sci.* **2010**, *35*, 1217. (c) H. Tian, Z. Tang, X. Zhuang, X. Chen and X. Jing, *Prog. Polym. Sci.* **2012**, *37*, 237.

[3] For a recent review, see Y. Wei, S. Wang and S. Zhou, *Dalton Trans.* **2016**, *45*, 4471.

[4] (a) N. Iwasa, M. Fujiki and K. Nomura, *J. Mol. Cat. A, Chem.* **2008**, *292*, 67; (b) C. Zhang and Z. -X. Wang, *J. Organomet. Chem.* **2008**, *613*, 3151; (c) N. Iwasa, J. Liu and K. Nomura, *Catal. Commun.* **2008**, *9*, 1148; (d) J. Liu, N. Iwasa and K. Nomura, *Dalton Trans.* **2008**, 3978; (e) N. Iwasa, S. Katao, J. Liu, M. Fujiki, Y. Furukawa and K. Nomura, *Organometallics,* **2009**, *28*, 2179; (f) N. Nomura, T. Aoyama, R. Ishii and T. Kondo, *Macromolecules,* **2005**, *38*, 5363; (g) D. Pappalardo, L. Annunziata and C. Pellecchia, *Macromolecules,* **2009**, *42*, 6056. (h) X. -F. Yu and Z. -X. Wang, *Dalton Trans*. **2013**, *42*, 3860. (i) T. -L. Huang and C. -T. Chen. *J. Organomet. Chem.* **2013**, *725*, 15. (j) A. Meduri, T. Fuoco, M. Lamberti, C. Pellecchia and D. Pappalardo, *Macromolecules*, **2014**, *47*, 534. (k) B. Gao, D. Li, X. Li, R. Duan, X. Pang, Y. Cui, Q. Duan and X. Chen, *Cat. Sci & Tech.* **2015**, *5*, 4644.

[5] Of 343 hits for dialkylaluminium where N and O complete the coordination environment, 76 contained chelating phenoxyimine as of November 2016. F. H. Allen, *Acta Crystallogr., Sect. B: Struct. Sci.*, **2002**, *58*, 380.

[6] For ROP of cyclic esters utilising aluminium phenoxyimine catalysts (see also table S1, SI), see: (a) S. M. Kirk, H. C. Quilter, A. Buchard, L. H. Thomas, G. Kociok-Kohn and M. D. Jones, *Dalton Trans.* **2016**, *45*, 13846. (b) B. Gao, D. Li, X. Li, R. Duan, X. Pang, Y. Cui, Q. Duan and X. Chen, *Cat. Sci. & Tech.* **2015**, *5*, 4644. (c) M. F. N. Iwasa, K. Nomura, *J. Mol. Cat. A* **2008**, *292*, 67. (d) H. -L. Chen, S. Dutta, P. -Y. Huang and C. -C. Lin, *Organometallics* **2012**, *31*, 2016. (e) N. Iwasa, S. Katao, J. Liu, M. Fujiki, Y. Furukawa and K. Nomura, *Organometallics* **2009**, *28*, 2179. (f) J. Yang, Y. Yu, Q. Li, Y. Li and A. Cao, *J. Polym. Sci. A: Polym. Chem.* **2005**, *43*, 373. (g) E. L. Whitelaw, G. Loraine, M. F. Mahon and M. D. Jones, *Dalton Trans.* **2011**, *40*, 11469. (h) D. J. Darensbourg and O. Karroonnirun, *Organometallics* **2010**, *29*, 5627. (i) W. Zhang, Y. Wang, W. -H. Sun, L. Wang and C. Redshaw, *Dalton Trans.* **2012**, *41*, 11587. (j) C. Zhang and Z.-X. Wang, *J. Organomet. Chem.* **2008**, *693*, 3151. (k) C. Di Iulio, M. D. Jones and M. F. Mahon, *J. Organomet. Chem.* **2012**, *718*, 96. (l) C. Agatemor, A. E. Arnold, E. D. Cross, A. Decken and M. P. Shaver, *J. Organomet. Chem.* **2013**, *745*, 335. (m) Z. Tang, X. Chen, X. Pang, Y. Yang, X. Zhang and X. Jing, *Biomacromolecules* **2004**, *5*, 965-970. (n) X. -F. Yu and Z.-X. Wang, *Dalton Trans.* **2013**, *42*, 3860. (o) H. -L. Han, Y. Liu, J. -Y. Liu, K. Nomura and Y. -S. Li,

Dalton Trans. **2013**, *42*, 12346. (p) B. Gao, R. Duan, X. Pang, X. Li, Z. Qu, Z. Tang, X. Zhuang and X. Chen, *Organometallics* **2013**, *32*, 5435. (q) I. Taden, H. -C. Kang, W. Massa and J. Okuda, *J. Organomet. Chem.* **1997**, *540*, 189. (r) S. L. Hancock, M. F. Mahon and M. D. Jones, *New J. Chem.* **2013**, *37*, 1996. (s) N. Zhao, Q. Wang, G. Hou, H. Song and G. Zi, *Inorg. Chimica Acta* **2014**, *413*, 128. (t) A. Arbaoui, C. Redshaw and D. L. Hughes, *Chem. Commun.* **2008**, 4717. (u) A. Alaaeddine, C. M. Thomas, T. Roisnel and J. -F. Carpentier, *Organometallics* **2009**, *28*, 1469. (v) M. Normand, T. Roisnel, J. -F. Carpentier and E. Kirillov, *Chem. Commun.* **2013**, *49*, 11692. (w) C. Kan, J. Ge and H. Ma, *Dalton Trans.* **2016**, *45*, 6682. (x) P. Hornnirun, E. L. Marshall, V. C. Gibson, R. I. Pugh and A. J. P. White, *Proc. Nat. Acad. Sci.* **2006**, *103*, 15343. (y) P. A. Cameron, D. Jhurry, V. C. Gibson, A. J. P. White, D. J. Williams and S. Williams, *Macromol. Rapid Commun.* **1999**, *20*, 616. (z) M. –C. Chang, W. –Y. Lu, H. –Y. Chang, Y. –C. Lai, M. Y. Chiang, H. –Y. Chen and H. –Y. Chen. *Inorg. Chem.* **2015**, *54*, 11292.

[7] N. Iwasa, J. Liu and K. Nomura, *Cat. Commun.* **2008**, *9*, 1148.

[8] J. Ma, K. -Q. Zhao, M. Walton, J. A. Wright, J. W. A. Frese, M. R. J. Elsegood, Q. Xing, W. -H. Sun and C. Redshaw, *Dalton Trans.* **2014**, *43*, 8300.

[9] M. Braun, *Angew Chemie.* **1996**, *108*, 565; *Angew Chemie. Int. Ed.* **1996**, *35*, 519.

[10] P. A. Cameron, V. C. Gibson, C. Redshaw, J. A. Segal, M. D. Bruce, A. J. P. White and D. J. Williams, *Dalton Trans.* **1999**, 1883.

[11] S. Milione, F. Grisi, R. Centore and A. Tuzi, *Eur. J. Inorg. Chem.* **2008**, 5532.

[12] V. C. Gibson, D. Nienhius, C. Redshaw, A. J. P. White and D. J. Williams, *Dalton Trans.* **2004**, 1761.

[13] (a) C. Redshaw, V. C. Gibson, M. R. J. Elsegood and W. Clegg, *Chem. Commun.* **2007**, 1951. (b) M. Lappert, A. Protchenko and P. Power in metal Amide Chemistry, Wiley and Sons, **2008**. (c) X. –F. Yu and Z. –X. Wang, *Dalton Trans.* **2013**, *42*, 3860.

[14] J. A. Hatnean, J. W. Thomson, P. A. Chase and D. W. Stephan, *Chem. Commun.* **2014**, *50*, 301.

[15] (a) W. Clegg, M. R. J. Elsegood, S. J. Teat, C. Redshaw and V. C. Gibson, *J. Chem. Soc., Dalton Trans.* **1998**, 3037. (b) W. Clegg, *J. Chem. Soc., Dalton Trans.* **2000**, 3223.

[16] For structurally characterized examples of Al – Me – Al bridges, see (a) R.V. Vranka and E. L. Amma *J. Am. Chem. Soc.* **1967**, *89*, 3121. (b) V. R. Magnuson, G. D. Stucky, *J. Am. Chem. Soc.,* **1969**, *91*, 2544. (c) S. K. Byram, J. K. Fawcett, S. C. Nyburg and R. J. O'Brien, *J. Chem. Soc. D.* **1970**, 16. (d) J. C. Huffman and W. E. Streib, *J. Chem. Soc. D.*1971, 911. (e) W. J. Evans, R. Anwander and J. W. Zille, *Organometallics,* **1995**, *14*, 1107. (f) S. D. Waezsada, F. -Q. Liu, E. F. Murphy, H. W. Roesky, M. Teichert, I. Uson, H.-G. Schmidt, T. Albers, E. Parisini and M. Noltemeyer, *Organometallics,* **1997**, *16*, 1260. (g) S. D. Waezsada, C. Rennekamp, H. W. Roesky, C. Ropken and E. Parisini, *Z. Anorg. Allg. Chem.* **1998**, *624*, 987. (h) W. T. Klooster, R. S. Lu, R. Anwander, W. J. Evans, T. F. Koetzle and R. Bau, *Angew. Chem., Int. Ed.* **1998**, *37*, 1268. (i) E. Ihara, V. G. Young Jr. and R. F. Jordan, *J. Am. Chem. Soc.* **1998**, *120*, 8277. (j) R. Wochele, W. Schwarz, K. W. Klinkhammer, K. Locke and J. Weidlein, *Z. Anorg. Allg. Chem.* **2000**, *626*, 1963. (k) J. E. Kickham, F. Guerin, J. C. Stewart and D. W. Stephan, *Angew Chem. Int. Ed.* **2000**, *39*, 3263. (l) Z. Yu, J. M. Wittbrodt, M. J. Heeg, H. B. Schlegel and C. H. Winter, *J. Am. Chem. Soc.* **2000**, *122*, 9338. (m) J. Klosin, G. R. Roof, E. Y. –X. Chen and K. A. Abbound, *Organometallics,*

2000, *19*, 4684. (n) E. Y. –X. Chen and K. A. Abbound, *Organometallics,* **2000**, *19*, 5541. (o) A. Cottone III and M. J. Scott, *Organometallics,* **2000**, *19*, 5254. (p) J. E. Kickham, F. Guerin, J. C. Stewart, E. Urbanska and D. W. Stephan, *Organometallics,* **2001**, *20*, 1175. (q) A. Cottone III and M. J. Scott, *Organometallics,* **2002**, *21*, 3610. (r) G. S. Hair, A. H. Cowley, J. D. Gorden, J. N. Jones, R. A. Jones and C. L. B. Macdonald, *Chem. Commun.* **2003**, 424. (s) A. J. R. Son, M. G. Thorn, P. E. Fanwick and I. P. Rothwell, *Organometallics,* **2003**, *22*, 2318. (t) B. C. Bailey, A. R. Fout, H. Fan, J. Tomaszewski, J. C. Huffman, J. B. Gary, M. J. A. Johnson and D. J. Mindiola, *J. Am. Chem. Soc.*, **2007**, *129*, 2234. (u) G. B. Nikiforov, H. W. Roesky, B. C. Heisen, C. Grosse and R. B. Oswald, *Organometallics,* **2008**, *27*, 2544. (v) H. M. Dietrich, J. W. Ziller, R. Anwander and W. J. Evans, *Organometallics,* **2009**, *28*, 1173. (w) A. –L. Schmitt, G. Schnee, R. Welter and S. Dagorne, *Chem. Commun.* **2010**, *46*, 2480. (x) A. Heman-Gomez, A. Martin, M. Mena and C. Santamaria, *Inorg. Chem.* **2010**, *49*, 8401. (y) G. Occhipinti, C. Meermann, H. M. Dietrich, R. Litlabo, F. Auras, K. W. Tomroos, C. Maichle-Mossmer, V. R. Jensen and R. Anwander, *J. Am. Chem. Soc.* **2011**, *133*, 6323. (z) N. Dettenrieder, H. M. Dietrich, C. Schadle, C. C. Maichle-Mossmer, K. W. Tomroos and R. Anwander, *Angew. Chem., Int. Ed.* **2012**, *51*, 4461.

[17] (a) S. Hamidi, H. M. Dietrich, D. Werner, L. N. Jende, C. Maichle-Mossmer, K. W. Tomroos, G. B. Deacon, P. C. Junk and R. Anwander, *Eur. J. Inorg. Chem.* **2013**, 2460. (b) G. Theurkauff, A. Bondon, V. Dorcet, J. –F. Carpentier and E. Kirillov, *Angew Chem. Int. Ed.* **2015**, *54*, 6343. (c) H. G. Stammler, S. Blomeyer, R. J. F. Berger and N. W. Mitzel, *Angew Chem. Int. Ed.* **2015**, *54*, 13816.

[18] (a) Y. Li, K. –Q. Zhao, M. R. J. Elsegood, T. J. Prior, X. Sun, S. Mo and C. Redshaw, *Cat. Sci.*

& Tech. **2014**, *4*, 3025.(b) Y. –C. Chen, C. –Y. lin, C. –Y. Li, J. –H. Huang, L. –C. Chang and T. –Y. Lee, *Chem. Eur. J.* **2008**, *14*, 9747.

[19] (a) N. Iwasa, S. Katao, J. liu, M. Fujiki, Y. Furukawa and K. Nomura, *Organometallics* **2009**, *28*, 2179. (b) D. Li, Y. Peng, C. Geng, K. Liu and D. Kong, *Dalton Trans.* **2013**, *42*, 11295. (c) W. –L. Kong, Z. –Y. Chai and Z. –X. Wang, *Dalton Trans.* **2014**, *43*, 14470. (d) W. Zhang, Y. Wang, L. Wang, C. Redshaw and W. –H. Sun, *J. Organomet. Chem.* **2014**, *750*, 65.

[20] M. J. Walton, S. J. Lancaster and C. Redshaw, *ChemCatChem.* **2014**, *6*, 1892 and references therein.

[21] (a) J. –C. Buffet and J. Okuda, *Chem. Commun.* **2011**, *47*, 4796. (b) P. Piromjitpong, P. Ratanapanee, W. Thumrongpatanaraks, P. Kongsaeree and K. Phomphrai, *Dalton Trans.* **2012**, *41*, 12704.

[22] Y. Liu, W. -S. Dong, J. -Y. Liu and Y. -S. Li, *Dalton Trans.* **2014**, *43*, 2244.

[23] S. Sriputtirat, W. Boonkong, S. Pengprecha, A. Petsom and N. Thongchul, *Adv. Chem. Eng. Sci.* **2012**, *2*, 15.

[24] See Handbook of Ring-Opening Polymerization, **2009**, Wiley-VCH, Eds. P.Dubois, O. Coulembier and J. –M. Raquez.

[25] M. K. Cooper, J. M. Downes, P. A. Duckworth, M. C. Kerby, R. J. Powell and M. D. Soucek, *Inorg. Synth.* **1989**, *25*, 129.

[26] (a) G. M. Sheldrick, *Acta Crystallogr.* **2008**, *A64*, 112; (b) G.M. Sheldrick, *Acta Cryst.* **2015**, *A71*, 3.

[27] G. M. Sheldrick, *Acta Cryst.* **2015**, *C71*, 3.

[28] G.M. Sheldrick, SHELXTL user manual, version 6.10. Bruker AXS Inc., Madison, WI, USA, (**2000**).

[29] SMART (**2001**), SAINT (**2001** & **2008**), and APEX 2 (**2008**) software for CCD

diffractometers. Bruker AXS Inc., Madison, USA.

Table 1. ROP of ε-caprolactone using complexes **1 – 11** (not **2**).

Run	Cat	T (°C)	CL : M :BnOH	Time (h)	Conv^a (%)	$M_n{}^b{}_{,GPC}$	$M_{n,Cal}{}^c$	PDI^d
1	**1**	80	250 : 1:1	3	97	24690	27790	1.23
2	**1**	110	250 : 1:1	3	96	13340	27500	1.73
3	**1**	110	250 : 1:2	3	89	4670	12750	1.65
4	**3**	80	250 : 1:1	3	95	17340	27220	1.54
5	**3**	110	250 : 1:1	3	93	13480	26650	1.73
6	**3**	110	250 : 1:2	3	94	4150	13470	1.52
7	**4**	80	250 : 1:1	3	65	3660	18660	1.23
8	**4**	110	250 : 1:1	3	92	6300	26360	1.46
9	**5**	25	250 : 1:1	3	67	3840	19230	1.12
10	**5**	45	250 : 1:1	3	75	4690	21510	1.17
11	**5**	60	250 : 1:1	3	90	5650	25790	1.19
12	**5**	80	250 : 1:1	3	95	15830	27220	1.76
13	**5**	110	250 : 1:1	3	96	16050	27500	1.36
14	**5**	110	250 : 1:2	3	85	5120	12180	1.47
15	**6**	80	250 : 1:1	3	84	2500	24080	1.63
16	**6**	110	250 : 1:1	3	95	2770	27220	1.21
17	**7**	25	250 : 1:1	1	35	1180	10000	1.01
18	**7**	80	250 : 1:1	1	99.5	7120	28360	1.69
19	**7**	110	250 : 1:1	13min	100	10770	28650	1.81
20	**8**	80	250 : 1:1	3	80	---	---	---
21	**8**	110	250 : 1:1	1	99	4670	28360	1.52
22	**8**	110	250 : 1:1	3	99.7	10190	28560	1.60
23	**9**	25	250 : 1:1	1	65	2070	18660	1.11
24	**9**	80	250 : 1:1	1	98	7770	28070	1.28
25	**9**	110	250 : 1:1	5min	98	7690	28070	1.32
26	**9**	110	250 : 1:1	1	100	17240	28640	1.28
27	**9**	110	250 : 1:2	1	96	9000	13750	1.28
28	**10**	25	250 : 1:1	1	45	4950	12950	1.08
29	**10**	110	250 : 1:1	10min	100	29040	28640	1.63
30	**10**	110	250 : 1:2	1	93	3730	13270	1.19
31	**11**	25	250 : 1:1	1	94	10520	26930	1.12
32	**11**	110	250 : 1:1	3 min	100	27380	28640	1.66
33	**11**	110	250 : 1:2	1	95	5470	13610	1.95

Runs conducted in toluene using 0.05 mmol of catalyst; CL = ε-caprolactone. ^{a} Determined by ^{1}H NMR spectroscopy; ^{b} M_n GPC values corrected considering Mark-Houwink factors (0.56 poly(ε-caprolactone)) from polystyrene standards in THF. ^{c} Calculated from ([Monomer]$_0$/[OH]$_0$) × conv.(%) × Monomer molecular weight + Molecular weight of BnOH. ^{d} From GPC.

Table 2. ROP of *rac*-Lactide (*rac*-LA) using complexes **1-11**.

Run	Cat	T (°C)	[*rac*-LA] :[cat]:[BnOH]	Time (h)	Conv (%)[a]	$M_{n, GPC}$[b]	M_n, cal[c]	PDI
1	**1**	110	100 : 1:1	12	75	8770	10920	1.76
2	**1**	110	200 : 1:1	12	78	10180	22590	1.32
3	**2**	110	100:1:1	12	64	9800	9330	1.21
4	**3**	110	50:1:1	12	30	1560	2270	1.13
5	**3**	110	100 : 1:1	12	65	7480	9480	1.26
6	**3**	110	200 : 1:1	12	79	15050	22880	1.37
7	**3**	110	400 : 1:1	12	80	21240	46230	1.46
8	**3**	110	600 : 1:1	12	82	22950	70910	1.68
9	**3**	110	800 : 1:1	12	73	28660	84280	2.36
10	**3**	110	400 : 1:1	1	71	6600	41040	1.15
11	**3**	110	100 : 1:1	5	75	4260	10920	1.41
12	**3**	110	400 : 1:1	6	75	6010	43350	1.28
13	**3**	70	400 : 1:1	12	78	6750	45080	1.25
14	**4**	110	400 : 1:1	12	79	11060	45650	1.60
15	**5**	110	100 : 1:1	12	78	6750	11350	1.16
16	**5**	110	200 : 1:1	12	84	8280	24320	1.23
17	**5**	110	400 : 1:1	12	86	7640	49690	1.15
18	**6**	110	100:1:1	12	72	6530	10380	1.19
19	**7**	110	100:1:1	1	---	---	---	---
20	**7**	110	100:1:1	6	65	4370	9480	1.09
21	**7**	110	50:1:1	12	49	2260	3640	1.04
22	**7**	110	100:1:1	12	74	4370	10780	1.09
23	**7**	110	150:1:1	12	80	4520	17400	1.21
24	**7**	110	200:1:1	12	85	6870	24610	1.23
25	**8**	110	100:1:1	1	---	---	---	---
26	**8**	110	100:1:1	6	---	---	---	---
27	**8**	110	100:1:1	12	74	4270	10770	1.27
28	**9**	110	100:1:1	1	---	---	---	---
29	**9**	110	100:1:1	6	55	2810	8040	1.11
30	**9**	110	100:1:1	12	78	4680	11350	1.21
31	**10**	110	100:1:1	12	56	3870	8180	1.23
32	**11**	110	100:1:1	12	72	5330	10380	1.18
33	**11**	110	100:1:2	12	66	3270	4810	1.50

Runs conducted in toluene using 0.02 mmol of catalyst; [a] Determined by ^{1}H NMR spectroscopy; [b] M_n GPC values corrected considering Mark-Houwink factors (0.58 poly (*rac*-lactide)) from polystyrene standards in THF; [c] Calculated from ([Monomer]$_0$/[OH]$_0$) × conv.(%) × Monomer molecular weight.

Table 4. ROP of δ-valerolactone using Al complex **1-11**

Run[a]	Cat	δVL : BnOH :M	Time/h	Conv.%[b]	M_n[c]	$M_{n,Cal}$[d]	PDI[e]
1	**1**	100:1:1	12	34	1920	3510	1.35
2	**2**	100:1:1	12	20	1500	2110	1.23
3	**3**	100:1:1	12	89	3220	9010	1.29
4	**4**	100:1:1	12	60	1900	6110	1.35
5	**5**	100:1:1	6	---	---	---	---
6	**5**	100:1:1	12	97	2790	9820	1.75
7	**5**	50:1:1	24	77	2370	3960	1.43
8	**5**	100:1:1	24	98	3850	9920	1.36
9	**5**	150:1:1	24	97	5350	14680	1.73
10	**5**	200:1:1	24	98	8310	19710	1.38
11	**6**	100:1:1	12	---	500	---	1.03
12	**6**	100:1:1	24	90	3670	9120	1.38
13	**7**	100:1:1	12	72	2280	7310	1.44
14	**8**	100:1:1	12	50	1700	5110	1.13
15	**9**	100:1:1	12	---	510	---	1.01
16	**9**	100:1:1	24	80	4520	8120	1.32
17	**10**	100:1:1	12	---	---	---	---
18	**10**	100:1:1	24	99	7340	10020	1.1
19	**11**	100:1:1	12	---	---	---	---
20	**11**	100:1:1	24	88	3960	8920	1.52

[a] Runs conducted in toluene using 0.05 mmol of catalyst at 110 °C. [b] Determined by ^{1}H NMR spectroscopy; [c, e] Determined by GPC. [d] Calculated from $([Monomer]_0/[OH]_0) \times conv.(\%) \times$ Monomer molecular weight + Molecular weight of BnOH.

Table 7. Crystallographic data for pro-ligands **L³Hdpa** and **L³Hdpg** and complexes **5** and **7**

Compound	**L³Hdpa**	**L³Hdpg**	**5**	**7**
Formula	$C_{28}H_{33}NO$	$C_{28}H_{33}NO$	$C_{30}H_{38}AlNO$	$C_{30}H_{38}AlNO$
Formula weight	399.55	399.55	455.59	455.59
Crystal system	Triclinic	Monoclinic	Monoclinic	Triclinic
Space group	$P\bar{1}$	$P2_1/c$	$P2_1$	$P\bar{1}$
Unit cell dimensions				
a (Å)	10.0491(4)	19.264(5)	12.019(7)	10.4155(6)
b (Å)	11.8421(5)	5.9804(7)	9.329(2)	12.2889(7)
c (Å)	22.5152(9)	22.048(3)	12.761(6)	22.1595(13)
α (°)	86.153(3)	90	90	78.099(2)
β (°)	88.412(3)	111.594(15)	111.22(5)	80.513(2)
γ (°)	67.738(4)	90	90	80.731(2)
V (Å³)	2474.05(19)	2361.8(8)	1333.8(11)	2713.5(3)
Z	4	4	2	4
Temperature (K)	293(2)	150(2)	150(2)	160(2)
Wavelength (Å)	0.71073	0.71073	0.71073	0.71073
Calculated density (g.cm⁻³)	1.073	1.124	1.134	1.115
Absorption coefficient (mm⁻¹)	0.064	0.067	0.097	0.10
Transmission factors (min./max.)	0.716/1.000	0.955/0.979	0.977/0.986	0.936/0.978
Crystal size (mm³)	$0.7 \times 0.4 \times 0.2$	$0.45 \times 0.25 \times 0.05$	$0.28 \times 0.20 \times 0.19$	$0.70 \times 0.52 \times 0.23$
θ(max) (°)	29.226	25.235	25.331	28.865
Reflections measured	32360	8827	7484	20453
Unique reflections	11750	4231	7484	12306
R_{int}	0.0319	0.0620	0.1661	0.0183
Reflections with $F^2 > 2\sigma(F^2)$	6867	2051	3692	10043
Number of parameters	548	280	287	611
R_1 [$F^2 > 2\sigma(F^2)$]	0.0762	0.0494	0.1195	0.0464
wR_2 (all data)	0.2324	0.1135	0.3432	0.1186
GOOF, S	1.042	0.804	1.007	1.019
Largest difference peak and hole (e Å⁻³)	0.673 and –0.468	0.237 and –0.316	0.719 and –0.427	0.363 and –0.275

Table 7 con't. Crystallographic data for complexes **9**, **10** and **11·MeCN**

Compound	9	10	11·MeCN
Formula	$C_{25}H_{35}Al_3NP$	$C_{17}H_{25}Al_2N$	$C_{32}H_{39}Al_2N_3$
Formula weight	461.45	297.34	519.62
Crystal system	Triclinic	Monoclinic	Triclinic
Space group	$P\bar{1}$	$P2_1/n$	$P\bar{1}$
Unit cell dimensions			
a (Å)	8.7689(14)	12.9996(3)	11.13092(14)
b (Å)	12.714(2)	9.1655(2)	11.31747(15)
c (Å)	12.722(2)	14.6167(2)	14.07252(15)
α (°)	79.822(2)	90	104.6534(10)
β (°)	77.110(2)	91.416(2)	108.3655(11)
γ (°)	75.776(2)	90	105.3906(11)
V (Å^3)	1329.0(4)	1741.02(6)	1508.40(3)
Z	2	4	2
Temperature (K)	150(2)	100(2)	100(2)
Wavelength (Å)	0.6861	0.71073	0.71075
Calculated density (g.cm^{-3})	1.153	1.134	1.144
Absorption coefficient (mm^{-1})	0.193	0.158	0.12
Transmission factors (min./max.)	0.977/0.996	0.475/1.000	0.872/1.000
Crystal size (mm^3)	$0.12 \times 0.08 \times 0.02$	$0.24 \times 0.19 \times 0.10$	$0.19 \times 0.15 \times 0.10$
θ(max) (°)	29.349	27.483	27.482
Reflections measured	8760	25639	39175
Unique reflections	6934	6880	6903
R_{int}	0.0274	0.0136	0.0224
Reflections with $F^2 > 2\sigma(F^2)$	4786	6178	6628
Number of parameters	293	202	347
R_1 [$F^2 > 2\sigma(F^2)$]	0.0478	0.0700	0.0366
wR_2 (all data)	0.1339	0.2052	0.0958
GOOF, S	1.014	1.059	1.024
Largest difference peak and hole (e Å^{-3})	0.525 and –0.320	0.769 and –0.302	0.388 and –0.317